# A CFD Simulation of High Altitude Testing of the Cryogenic Engine

A Thesis submitted in Partial Fulfilment of the requirements for the degree of

**Master of Technology**
in
**Mechanical Engineering**

By
**Sk. Avez Shariq**


Department of Mechanical Engineering
National Institute of Technology
Rourkela
2016

# A CFD Simulation of High Altitude Testing of the Cryogenic Engine

A Thesis submitted in Partial Fulfilment of the requirements for the degree of

**Master of Technology**
in
**Mechanical Engineering**

By
**Sk. Avez Shariq**

Under the guidance of



**Prof. Sunil Kumar Sarangi**
Department of Mechanical Engineering
National Institute of Technology
Rourkela – 769 008

**Dr. V Narayanan**
Deputy Director / Project Director C-25
Liquid Propulsion Systems Centre, ISRO
Trivandrum – 695 547

**Dr. K. S. Biju Kumar**
Scientist – SG
Engine Fluid Systems and Analysis Division
Liquid Propulsion Systems Centre, ISRO
Trivandrum – 695 547

# Certificate

This is to certify that the dissertation, entitled "**A CFD Simulation of High Altitude Testing of the Cryogenic Engine**" is a bonafide work done by **Sk. Avez Shariq** under my close guidance and supervision in the Cryogenic Propulsion and Engines Group of **Liquid Propulsion Systems Centre, Valiamala, Trivandrum** for the partial fulfilment of the award for the degree of Master of Technology in Mechanical Engineering with specialization in Cryogenic and Vacuum Technology at **National Institute of Technology, Rourkela.**

The work has been executed here for a period of 1 year from May 2015 to April 2016, and to the best of my knowledge, has not been submitted to any university for the award of similar degree.

**Dr. K. S. Biju Kumar**
Scientist -SG
Engine Fluid systems and Analysis Division
Liquid Propulsions Systems Centre, ISRO
Trivandrum – 695 547

**Dr. V. Narayanan**
Deputy Director/
Project Director C-25
Liquid Propulsions Systems Centre, ISRO
Trivandrum – 695 547


# National Institute of Technology
# Rourkela

## Certificate

This is to certify that the thesis entitled, **"A CFD Simulation of High Altitude Testing of the Cryogenic Engine**" submitted by **Sk. Avez Shariq** in partial fulfilment of the requirements for the award of Master of Technology Degree in **Mechanical Engineering** with specialisation in "**Cryogenic and Vacuum Technology**" at the National Institute of Technology, Rourkela (Deemed University) is an authentic work carried out by him/her under my/our supervision and guidance.

To the best of my knowledge, the matter embodied in the thesis has not been submitted to any other University/ Institute for the award of any degree or diploma.

**Prof. Sunil Kumar Sarangi**
Department of Mechanical Engineering
National Institute of Technology
Rourkela – 769 008

# Acknowledgement

**All praise be to the Almighty God, the creator of the Universe**

A heartfelt thanks to Prof. Sunil K. Sarangi, Director, NIT Rourkela and Dr. V. Naraynan, Deputy Director, LPSC, ISRO for having faith in me and permitting me to do my project at ISRO. I would like to thank the Director of LPSC, ISRO for providing facilities at LPSC. I would also like to thank my external guide Dr. K. S. Biju Kumar, Scientist-SG, ISRO for lending his intellectual prowess and his surplus resources to help me accomplish my task.

I would extend my sincere thanks to the faculty of NIT Rourkela whose impeccable lectures have enhanced my enthusiasm towards engineering and also made me worthy of the task given.

I am ever so grateful to my parents and my younger brother as their continuous motivation and support keeps transforming me into a better man.

I would also thank my cousin Atheequr Rehaman, Research scholar, Mining Engineering department, NIT Rourkela for encouraging me to join this audacious institute.

I thank all my friends especially K. N. Sai Manoj for making my stay very pleasant at NIT. I also thank my colleagues Basil George Thomas and Reetu Bharti for being supportive towards my project and who made it possible to enjoy my stay in Kerala.

A thanks wouldn't go amiss to the generations of researchers who have laid the foundations upon which I have done my work. I also thank my well wishers who have directly or indirectly contributed for my well being.

# Contents

# List of Figures and graphs

# Abstract

A rocket designed to operate in outer space will show deviation in performance when tested at sea level. This is because of the large back pressure (1 bar) acting on it. Therefore it is tested by simulating high altitude conditions in controlled environment called High Altitude Testing (HAT). This is necessary not only for testing and developing the Engine but also to fully qualify it to be integrated into the launch vehicle.

This report briefs about the design of a HAT facility. It presents a view on difficulties during CFD simulation and manual testing of the Engine. It provides a work-around for mesh interfacing of various parts. It shows how to select a suitable working fluid for the Ejector in order to create vacuum. It also shows the optimisation of mass flow rate of Nitrogen and Steam for the Ejector. It glimpses the Aero-Thermal behaviour of Nozzle flow with both Ejector On and Off conditions to prove self-pumping mode. It studies the Engine start up mode operation. It focusses on Engine shut down transient analysis. It also focusses on the re-entry of air into the facility during this process. It shows the role of Ejector in preventing re-entry of air and delaying flow separation in the Nozzle during this process.

# 1.1 Introduction

## 1.1.1 Prologue

“**Many people feel small, 'cause they're small and the Universe is big;**
**But I feel big because my atoms came from those stars.**”

**“And yes, every one of our body's atoms is traceable to the Big Bang and to the Thermonuclear furnace within high mass stars.”**

- Neil deGrasse Tyson
American Astrophysicist
Director of Hayden Planetarium
Rose Centre for Earth And Space, NYC

Ever since the inception of human life on Earth, mankind has always been curious about Space. It started with irrational thought by attributing celestial objects like the stars and comets to calamities on Earth. In the western world, it was believed that God sent Comets as a sign of destruction whenever a civilisation reached its pinnacle of sin. But when the era of Science dawned, they discovered that comets are only icy asteroids orbiting the sun just like the Earth is. So they used this Science to uncover all the hidden mysteries of earth and beyond its skies.

Today we have travelled to the moon and sent man-made satellites beyond the Heliosphere of the Sun. Such special missions requires special Space Transportation Systems (STS) like rockets and space shuttles which the mankind is still trying to master its creation. Many countries all over the globe have tried to build both expendable and re-usable STS s for over half a century.

There are several government agencies conducting space research among which, only a few have the full capability of launching rockets. They are

- China national space administration (CNSA)
- European Space Agency (ESA)
- Indian Space Research Organisation (ISRO)
- Japan Aerospace eXploration Agency (JAXA)
- National Aeronautical Space Administration (NASA)
- Russian Federal Space Administration (RFSA)

Out of them only NASA, RFSA, CNSA are capable of human space flight.

In India, the audacious ISRO has made many rockets for space exploration with the motto “**Space technology in the service of humankind**”. Apart from Sounding Rockets the other STS are

- **Satellite Launch Vehicle** (SLV) which has a range of 500 Km has the capacity of 40 Kg

- **Augmented Satellite Launch Vehicle** (ASLV) which has the capacity to carry a pay-load of 150 Kg
- **Polar Satellite Launch Vehicle** (PSLV) whose versatility can be demonstrated by mentioning a fact that the PSLV – C9 was used to launch as many as 10 satellites at a time on 28 April 2008
- **Geosynchronous Satellite Launch Vehicle** (GSLV) in which the indigenously developed Cryogenic Upper Stage (CUS) was used aboard the GSLV – D5 flight on 5 Jan '14.
- **Geosynchronous Satellite Launch Vehicle, Mark III** (GSLV Mk III) which has the capacity to lift 4 Tonnes and has been rightfully called the “Monster Rocket of India”. It has 2 strap-on solid booster rockets unlike the GSLV which has 4 liquid strapons. It is a 3 stage rocket with the final stage (C-25) being Cryogenic.

### 1.1.2 C-25 Stage

This stage provides half of the velocity required for achieving a Geosynchronous Transfer Orbit. It uses a liquid Oxygen and liquid Hydrogen as the propellant combination (these are Cryogenic fuels unlike Earth storable fuels that are used in initial stage of the rocket). The 27 tonne propellant burns for 640s and delivers a thrust of 200 KN. The CE20 Engine uses independent Turbo-Pumps and a regeneratively cooled Thrust Chamber. It works on the “Gas Generator” Propulsion cycle.

## 1.2 Rocket Propulsion cycles

Broadly speaking there are three commonly used cycles in rocket propulsion. They are

- Staged Combustion cycle
- Gas Generator cycle
- Expander cycle

### 1.2.1 The Staged Combustion cycle

This is a closed cycle. Here the fuel is partially burned after regeneration and used to run the turbo-pumps. Then the partially combusted gas is admitted to the Thrust chamber. Therefore high power Turbo-Pumps are used. This gives us very high chamber pressures and high expansion nozzles can be used. On a whole and excellent performance is delivered. But, this results in harsh environments to the turbine. It also requires complex hot gas plumbing and feed back control. Such high pressures cause corrosion if oxidiser rich conditions exist and this require expertise in advanced Metallurgy.

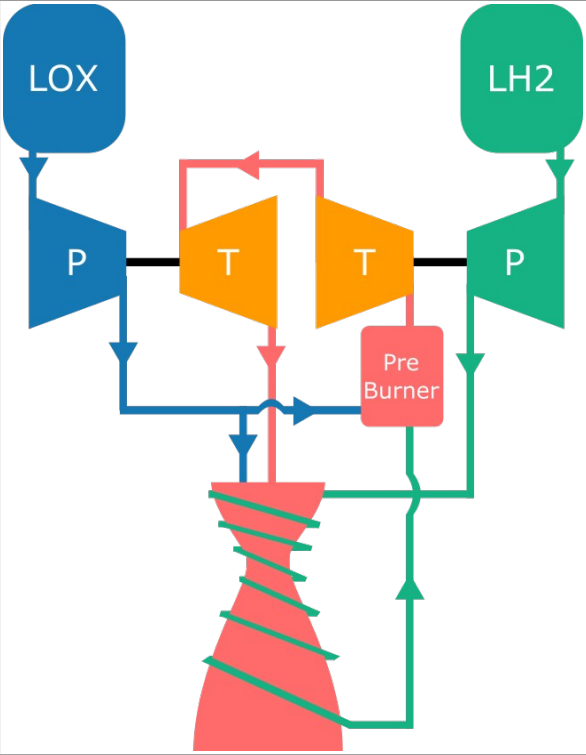


**Figure 1-1: Staged Combustion cycle**

### 1.2.2 The gas Generator cycle

The rocket fuel (in this case liquid Hydrogen (LH2)) is fed to the fuel compressor. The compressed fuel is circulated in the walls of nozzle for regeneration. This also serves the purpose of cooling down the nozzle. After regeneration the Propellant is fed to the nozzle for combustion.

A part of the fuel coming from the compressor is fed to a Gas Generator (GG). Here also combustion occurs but the product gas is sent to a turbine that drives the Propellant compressor. After that the product gas is used to drive the turbine that drives the Oxidiser compressor (in this case Liquid Oxygen(LOX)). From there it is vented out into space.

On the other hand the oxidiser flows to its corresponding compressor, which is being driven by a turbine. From there a part of it flows to Gas Generator while the remaining part flows to the Thrust Chamber for combustion.

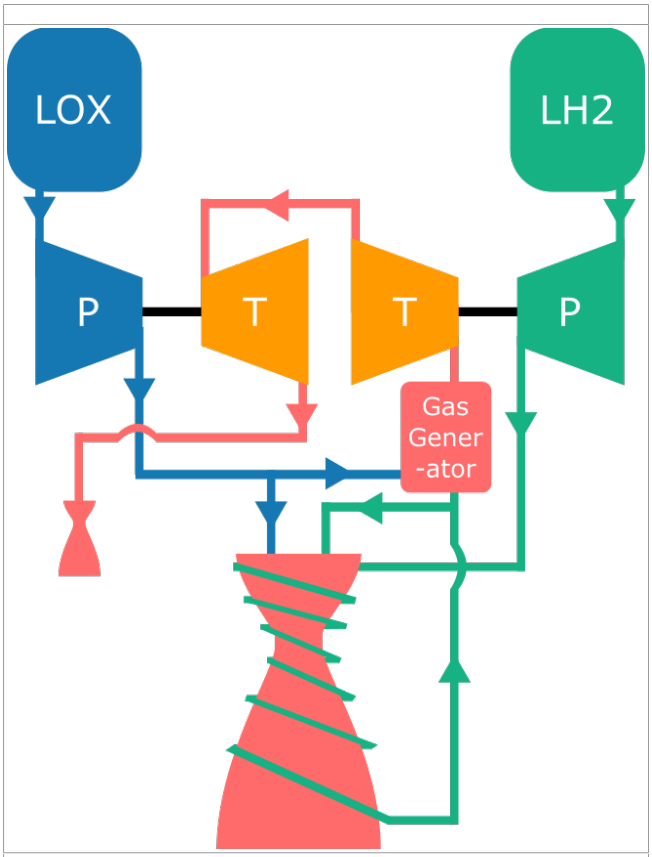


**Figure 1-2: Gas generator cycle**

It is an open cycle. An independent line of fuel and oxidiser is run to the Gas Generator where complete combustion occurs and the exhaust gas is used to power the Turbo-Pumps. Another independent line runs from the tanks to the Thrust chamber. Therefore these lines can be designed to run at different pressures giving flexibility. Therefore plumbing of gas and design of feed lines is simple. The engine is less expensive and lighter. Being an open cycle some of the propellant is lost which decreases the propellant efficiency. But this loss is compensated by spraying the lost propellant on the nozzle for additional cooling.

### 1.2.3 The Expander cycle

The expander cycle is a simple rocket propulsion cycle where propellant from the tank is regenerated to change phase from liquid to gas and then admitted into the Thrust chamber. The Oxidiser is directly admitted to the Thrust chamber. However it has limitations. The Thrust is limited by the expansion ratio of the nozzle. As the surface area of the nozzle changes (to increase the expansion ratio) the amount of propellant regenerating also changes. So the Thrust is limited by square cube rule (as the surface area increases the volume of fuel getting regenerated increases to the cubic power of radius of nozzle). Theoretically there exists a maximum value beyond which a by-pass expander is required to further increase the thrust.

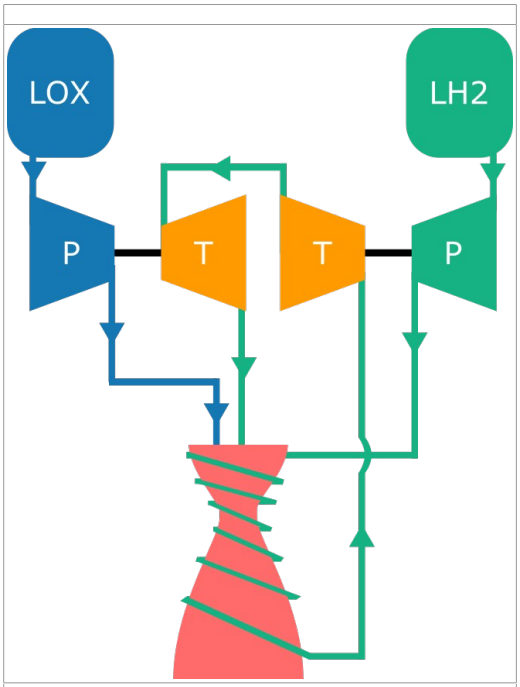


**Figure 1-3: Expander cycle**

The Expander cycle is the basic among all the cycles. The staged combustion cycle delivers maximum thrust. But it is also common to use Gas generator cycle owing to its ease of design. Each pressure line can be designed and tested separately. This increases its flexibility.

When the combustion gas completes the cycle, it is expelled through a Nozzle. This Nozzle is responsible for thrust generated by the rocket. The thrust depends mainly on the temperature and exit velocity of the flow. The temperature is achieved by combustion of gases. The flow velocity is achieved by its geometry.

## 1.3 Nozzle characteristics

### 1.3.1 A De-Laval Nozzle

A flow can reach supersonic speeds only by being accelerated in a De-Laval nozzle. Considering this throttling to be isentropic, we can say that the Potential energy (Pressure head) is converted to Kinetic energy. Thus the pressure at the exit of the nozzle is very less.

Let us consider a De-Laval nozzle with inlet pressure $P_i$. Its exit is maintained in a chamber of constant pressure. This is usually termed as Back Pressure / Ambient Pressure $P_b$. Let the pressure developed at the throat cross-section of the nozzle be $P_t$. The pressure developed at the exit of the nozzle is $P_e$. It is to be noted that the exit pressure may not always be equal to the back pressure. That is why a separate notation has been used.

When the ambient conditions are altered, the following have been observed

- If the inlet conditions are the same as the ambient conditions then there is no driving force to create a flow in the nozzle.

- When the back pressure is reduced we see the pressure characteristics depicted by line AG as shown in the figure below. Here the flow starts, and it accelerates up to the throat which acts as a nozzle to it. But then it decelerates in the Diffuser section.
- Further reducing the back pressure we see that the flow further accelerates and can be seen by the lines AF and AE. It is to be noted that the flow has reached sonic conditions at the throat as shown by AE.
- Further reducing the back pressure do not show the same characteristics as earlier. The pressure characteristics are shown by the line AD. It can be noticed that an abrupt change in pressure somewhere in the Diffuser section is caused. This is called a 'shock'. Because of a shock the pressure rises making the flow subsonic. So after the shock, the diverging portion acts as a Diffuser and slows down the flow. But before the shock, this portion acts as a nozzle to the supersonic flow thus increasing the speed of flow. Once the flow reaches sonic conditions in the throat, the mass flow rate remains the same no matter how large the pressure difference becomes. Then the flow is said to be 'chocked'.
- Further reducing the back pressure we see the that the shock travels towards the exit of the nozzle. This can be seen in AC and AB.
- There exists a point when the shock is completely outside the nozzle. This line is AO. This is called the design line. All nozzles delivering high performance are designed based on this line[1].

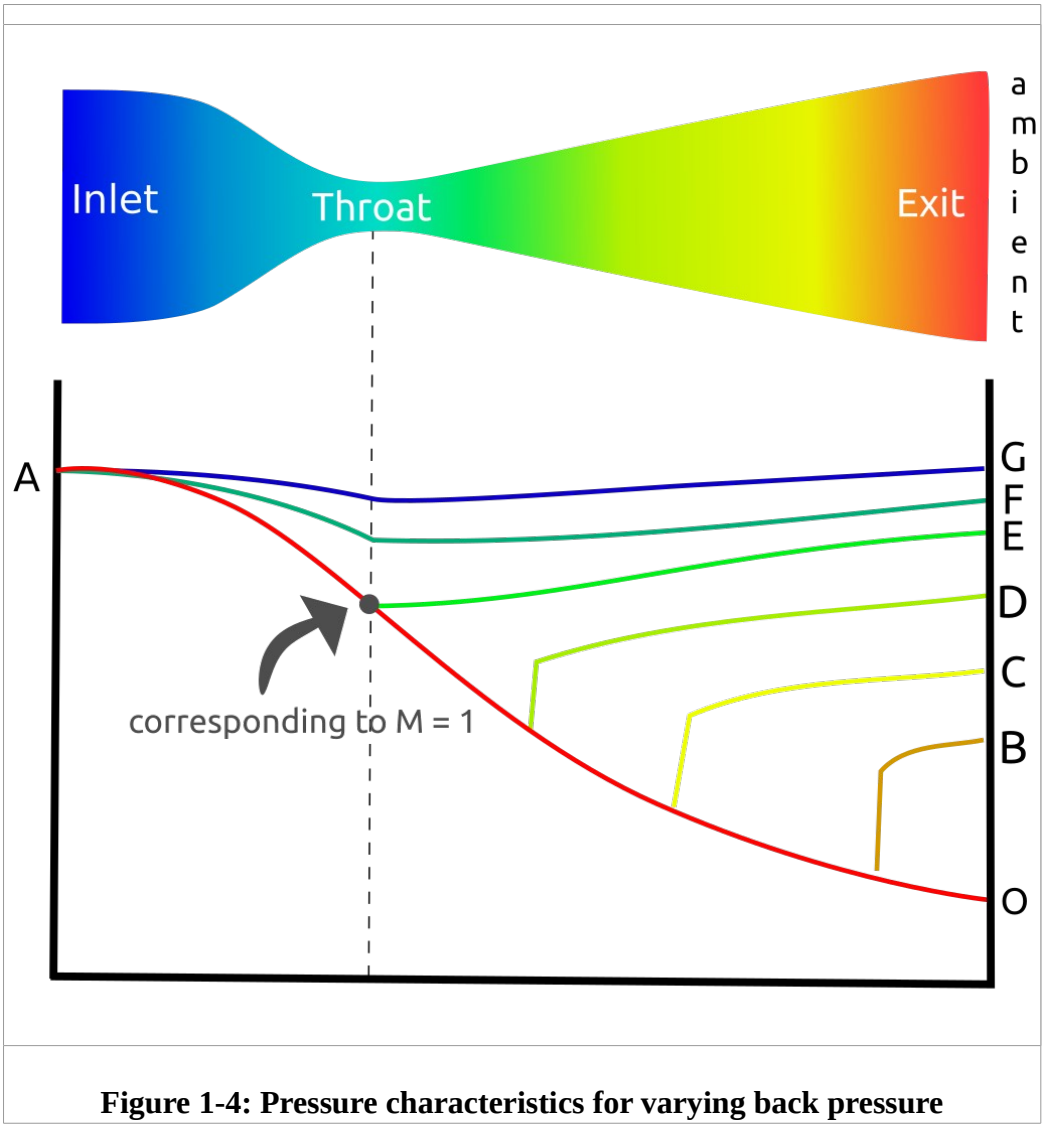


**Figure 1-4: Pressure characteristics for varying back pressure**

### 1.3.2 Improper expansion

As it was mentioned that the line AO is the design criteria for the area expansion ratio of a nozzle, then it is obvious that when the nozzle is designed for such conditions it behaves differently at different back pressure. This brings us to the general concept of Under-expansion and Over expansion.

When the Nozzle exit pressure equals to that of the surroundings, then the expansion is normal. It is ideal form of expansion and there is no pressure loss. The exhaust plume then diffuses into the air due to concentration difference and not due to any pressure gradients. Figure 1-5 shows a representation of normal expansion.

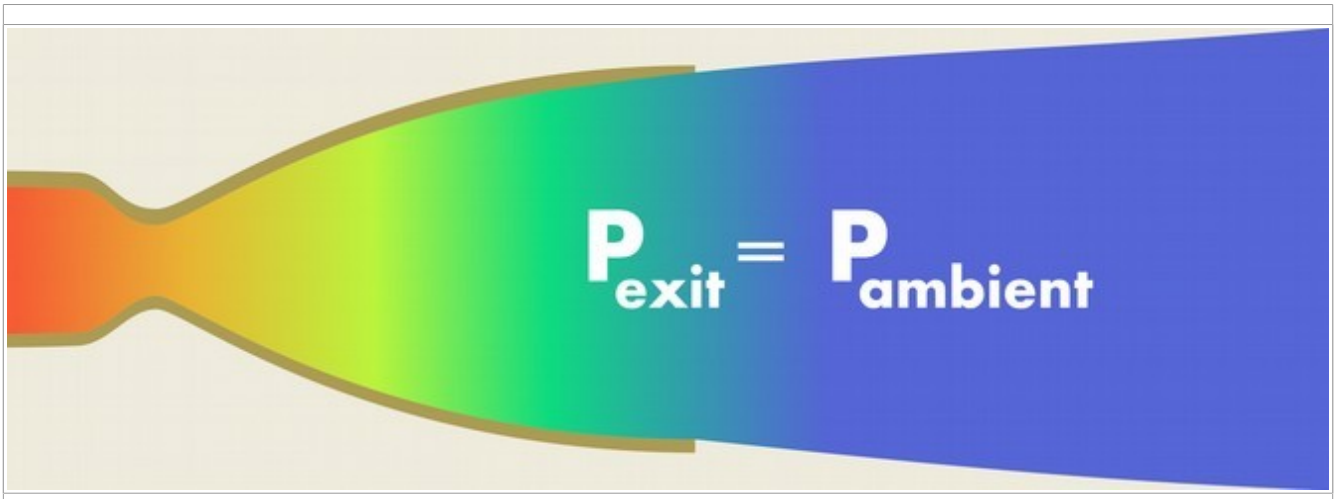


**Figure 1-5: Normal Expansion**

When the nozzle exit pressure is greater than the back pressure then it means that the flow has not expanded to the full capacity to match the surroundings. This means that the flow is Under-expanded. Because of this, the flow expands immediately when it reaches the exit of Nozzle and diffuses into air. Large pressure gradients are formed. Since the flow is not expanded to its full potential the efficiency is less. This is a general case when the Nozzle is designed for sea level and operated in vacuum. Figure 1-6 shows a representation of Under expansion.

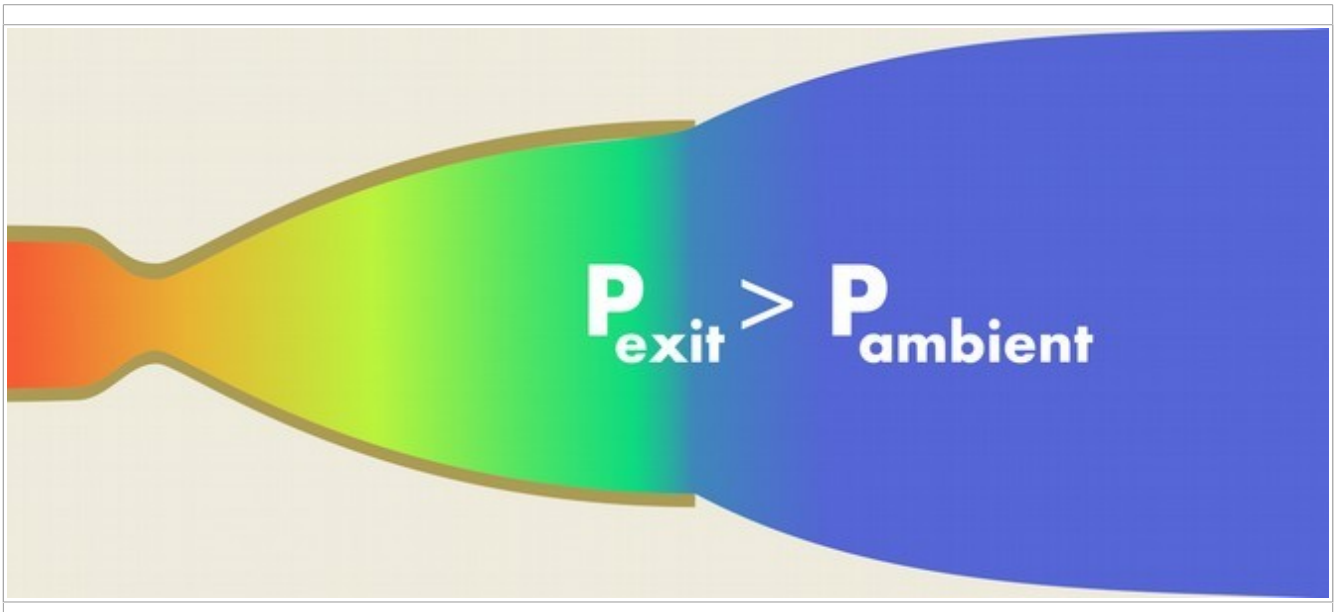


**Figure 1-6: Under Expansion**

When the nozzle exit pressure is lesser than the back pressure then the flow has expanded beyond what is required. Hence this flow is over-expanded[1]. Since the flow is over expanded the pressure at the exit plane is less than that of ambient. This provides the ambient air to back flow into

the nozzle forming small pockets of recirculation zone. At these zones the flow is detached from the walls. The separated part of nozzle is not useful for expansion and is only an additional weight. This decreases the thrust to weight ratio and thus its efficiency. This is a general case when Nozzle is designed for vacuum but operated at sea level. Figure 1-7 is a representation of over expansion.

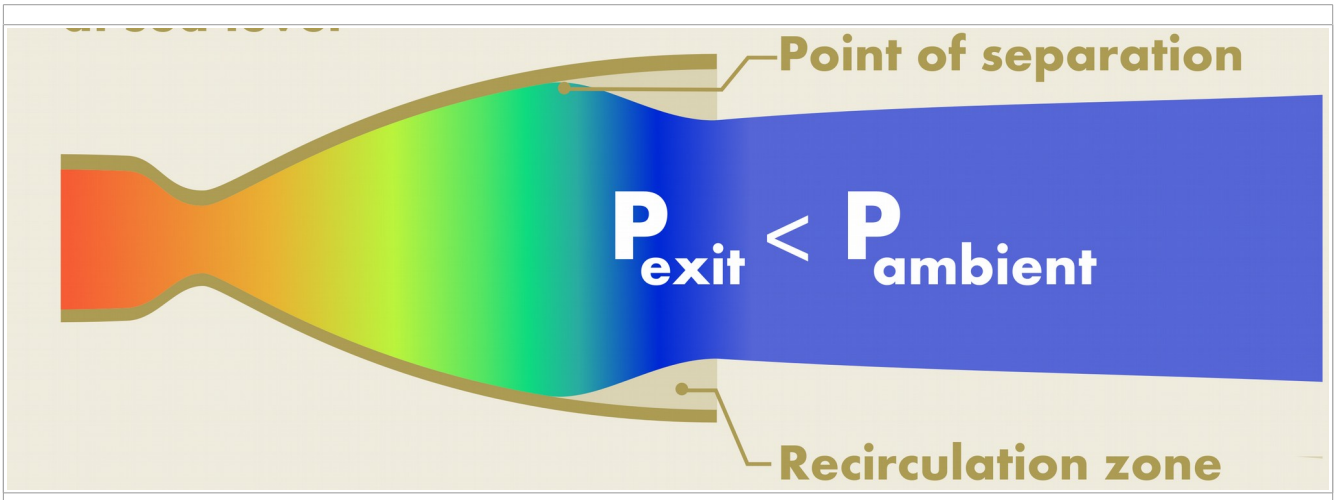


**Figure 1-7: Over Expansion**

### 1.3.3 Over expansion and flow separation

Over-expansion is dangerous during operation. When a large pressure gradient is formed on the boundary layer then the layer cannot keep up with it. It splits from the walls of the nozzle. This is called ' nozzle flow separation '[2]. It creates asymmetric radial loads for a brief period of time. But it can cause damage to the nozzle[1]. It shall be pointed out that flow separation is not the immediate consequence of Over-expansion. It is usually after 40 % of over-expansion that the flow separation can be seen. Although no definite mathematical formula exist for predicting flow separation, there are a lot of correlations from experimental studies that suggest the zone of safety. That is why an additional margin of 20 % is recommended form the results obtained from them[3].

The best solution to avoid this problem is to avoid flow separation. It has been discussed that flow separation occurs in cases where the rocket engine is designed for operation in outer space is tested at sea level. Hence a test facility can be created to simulate outer space conditions (essentially vacuum pressures). This is called High Altitude Test facility (HAT).

## 1.4 High Altitude Test facility

The facility consists of a large Vacuum chamber where the rocket motor is to be placed for testing. Air is evacuated from this chamber to simulate high altitude conditions. A traditional Ejector system is employed to make full flow in the Nozzle. The Ejector system creates vacuum by entraining the ambient air molecules present in the Vacuum chamber into the rapidly flowing

working fluid of the Ejector. Typically very high flow rates of Ejector fluid are required.

The rocket nozzle converts all energy (including Pressure energy) into high Mach flow. The pressure of this flow is very less. An Ejector has to be designed to create pressures less than this value, which is not possible in most cases. Unless this is done, flow from the Ejector flows into the Nozzle and causes mixing. Thus a pressure recovery system is required and that is done by the Diffuser section. The water cooling is used to bring down the temperature of exhaust gases[4].

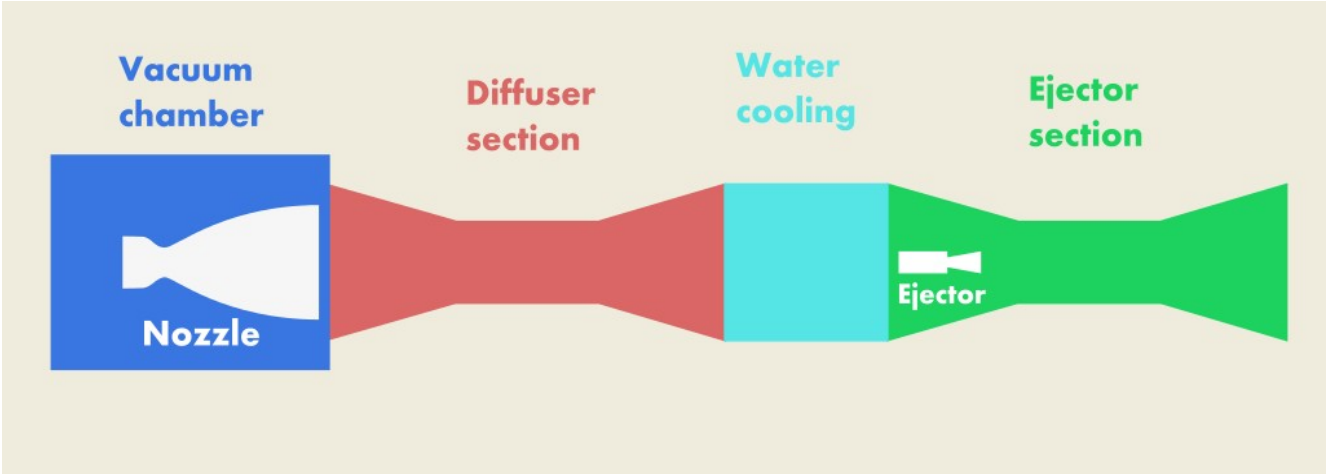


**Figure 1-8: A representation of High Altitude Test facility**

## 1.5 Motivation of the Project

LPSC is developing a High Thrust Cryogenic Engine for the third stage of GSLV MkIII. The development tests of the Engine are completed at Sea level using a nozzle of area ratio 10. The next step is to test the full area ratio nozzle under Vacuum conditions using HAT facility. Previous studies indicate that Engine will work in Self-Pumping mode (a condition where the Ejector is switched off in the middle of the test where the exhaust coming from the rocket is sufficient to maintain vacuum in the Vacuum chamber) in the HAT facility. Hence the Ejector is switched off after the initial transient (the transient part where the rocket motor reaches from no-load to full-load condition). In case of test abort in between, there is a possibility of air entry to the Diffuser and spontaneous reaction inside the Diffuser. This will damage the hardware and the facility. For understanding the Aero-Thermal behaviour under this condition a detailed transient analysis is required.

## 1.6 Challenges of the HAT facility

- The HAT facility must be effectively sealed off to prevent air leaks

- Vacuum should always be maintained in Vacuum chamber
- Very large amounts of Ejector fluid is required
- Optimal design of Ejector and Ejector section is required
- Optimal design of Second throat (Diffuser section) is essential
- Cooling methods to protect Diffuser and Ejector systems

## 1.7 Major Objectives of the Project

- To optimise the Ejector flow rate
- To analyse Ejector operation under transient conditions
- To analyse Thrust chamber starting up under transient conditions
- To study Aero thermal behaviour under steady state conditions
- To study Aero thermal behaviour during Thrust chamber shut-down under transient conditions

# 2. Literature Survey

## 2.1 Prologue

High Altitude test facilities have been well implemented in many nations. In India, the ISRO (Indian Space Research Organisation) has carried out experiments to design a HAT facility that can be used to test the third stage motor of the PSLV (Polar Satellite Launch Vehicle). They use both Nitrogen gas and hot rocket exhaust gas as driving fluids in the facility[4]. Currently, HAT facilities are available for testing both Earth storable and Cryogenic engines.

In the US, experimental and theoretical analyses have been carried out at AEDC (Arnold Engineering Development Centre) to develop an equipment that can simulate high altitude conditions at ground level. This AEDC has proposed various theoretical methods to determine the starting conditions of a Diffuser[5].

In France, the DGA / CAEPE has developed a HAT facility named MESA. It consists of a vacuum pump, an Ejector and a Diffuser. Four Diffuser experiments were performed at the ONERA facility to find an optimum configuration. Here numerical analysis was used to evaluate experimental data collected at the facility[6].

At Purdue University a lab-scale facility was developed by employing an air powered Ejector and a blow off door for the initial low back pressure to the hybrid Rocket motor[7].

All major space exploration agencies have done considerable research in various aspects of design, testing, improving the HAT facility. Although the end result is generation of vacuum, it has been achieved in slightly different ways. For example NASA has employed Chemical Steam Generator to create steam via a chemical reaction whereas ESA injects water into rocket exhaust gases to vaporise it and use that steam. One more example is that NASA and ESA use multiple ejectors in parallel mode where as JAXA uses them in series. Hence it is essential to comprehend their techniques.

## 2.2 HAT facilities around the globe

### 2.2.1 NASA

Using the existing and proven technologies of the A-1 Test facility like the Propellant Run Systems, Propellant storage and transfer systems, Data acquisition, control, Instrumentation systems, infrastructure a new test facility is being built by NASA called the A-3 Test facility[8].

In US the driving fluid is primarily steam. They use a CSG (Chemical Steam Generator) instead of establishing a whole commercial steam plant. SSC (Stennis Space Centre) plans to use this technology to maintain HAT conditions in the A-3 facility. The initial cost of this CSG is far less than the steam plant. The added advantages are that

- They are capable of producing superheated steam with high flow rates
- They can produce steam very quickly

- They do not require staff of a licensed steam plant to operate the plant
- The rocket engine test conductors who are already employed at the ground test facility can handle the equipment with ease

This CSGs use Liquid Oxygen ( LOX) and Isopropyl Alcohol (IPA) as the propellants. It is proposed to use as many as 9 units in parallel to achieve the conditions to test the J-2X engine. The chemical reaction is[9]:

$$9\ O_2 + 2\ C_3H_8O \rightarrow 6\ CO_2 + 8\ H_2O$$

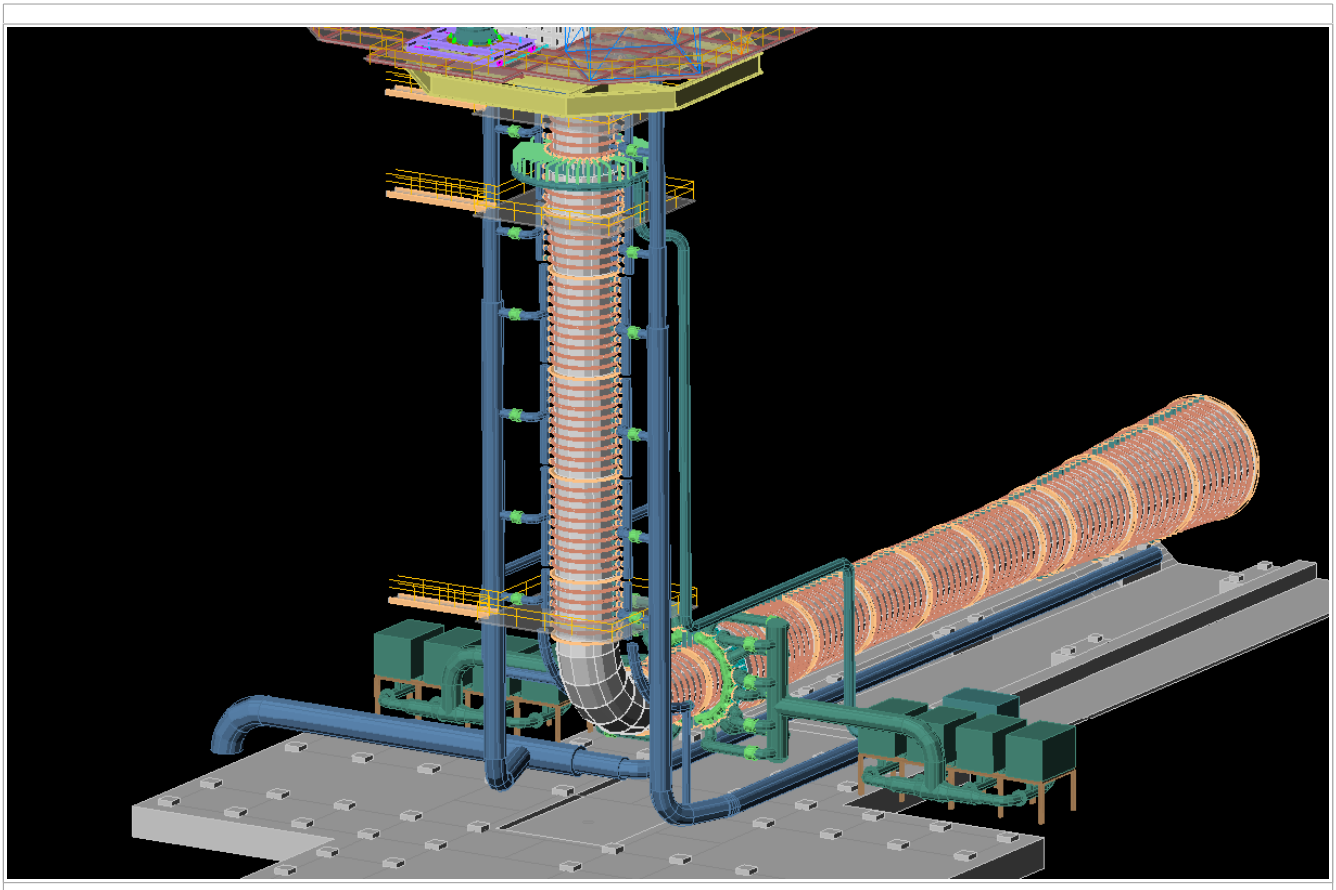

**Figure 2-1: A 3-D model of the A-3 Test stand**

At NASA's Glenn research test facility a B-2 facility has been developed. It is the only facility that is capable of testing a full scale upper stage launch vehicle and a rocket engine at HAT conditions. Here the engines or the vehicles can be exposed for indefinite period of time to low ambient pressures, low background temperatures, and dynamic solar heating, simulating the environment the hardware will encounter during orbital or interplanetary travel. Here vehicle engine systems producing up to 100,000 kb (~ 4536 Kg) of thrust can be fired for either single or multiple burn missions, utilising either cryogenic or storable fuels or oxidisers. This facility infrastructure is capable of being modified to test engine systems that can produce 400,000 kb (~ 181437 Kg) of thrust. Engine exhaust conditions can be controlled to simulate a launch ascent profile. In addition, altitude conditions can be maintained before, during, and after the test firing[10].

Currently NASA has 6 Test stands. The details are furnished below.

## Test stand 302

Test stand 302 is an insulated 32 ft diameter by 36 ft (10 m diameter by 11.6 m high) high carbon steel altitude chamber capable of holding propulsion systems up to approximately 64 Ft (19.5 m) in diameter. It has 3 interior levels for test article access.

Specifications:

- Single position, vertical firing capability
- Altitude capable to 30.5 km for engine firing with steam; up to 76 km non-firing with vacuum pumps
- Propellants: $N_2H_4$
- Propellant capability – 2800 gal hydrazine conditioning unit: Propellant can be saturated with He or $N_2$ up to 540 psia; propellant temperature conditioned between 4 to 49 $^0$c; 2000 gal hydrazine dump tank
- Maximum thrust – 111 kN
- Vacuum test chamber 10 m diameter by 11.6 m tall or 17.7 m with extension
- Removable lid for large test article installation

## Test stand 303

Test stand 303 is an insulated 3.35 m diameter by 11.9 m horizontal carbon steel altitude chamber capable of holding propulsion systems up to approximately 64 Ft (19.5 m) in diameter. It is capable of testing single engines or test articles with multiple engines up to 4.5 kN total thrust.

Specifications:

- Single position, horizontal test firing capability
- Altitude capability – 30.4 km for engine firing with steam system up to 76 km non-firing with vacuum pumps
- Propellants: $N_2H_4$
- Propellant capability – 2800 gal hydrazine conditioning unit: Propellant can be saturated with He or N2 up to 540 psia; propellant temperature conditioned between 4 to 49 $^0$c; 2000 gal hydrazine dump tank
- Maximum thrust – 4.5 kN
- Maximum test article size of 2 m diameter by 7.6 m long 150 psig nitrogen supplied
- Shares test cell 302 hydrazine system
- Currently testing APU

## Test stand 401

Test stand 401 is 9.75 m diameter by 10 m high carbon steel altitude capable of accommodating a vehicle with thrust vector control , 110 kN thrust engine firing vertically downward. The stand is capable of testing Max. test articles of 4.5 m x 4.6 x 13.7m. It has three interior levels which can be configured to meet the test requirements.

Specifications:

- Single position vertical firing capability
- Altitude test capability – 30.5 km for engine firing with steam systems up to 76+ km, not firing with vacuum pumps
- Propellants GO2, LH2, LOX, Hydrazine, $N_2O_4$ and hydrocarbon
- Propellant capability – 2000 gal storage per run time for hyperbolic propellants (MMH $N_2O_4$) can be saturated with He up to 600 psia; both propellants can be temperature conditioned between 4 and 49 $^0$c; pressure or pump transfer propellants; two propellant aspiration systems installed
- 500 gal, 600 psi hydrogen carbon fuel system.
- Max thrust 111 N vertical firing; screw jack precision test article positioning system; ambient pressure temperature conditioning form -1 $^0$c to 49 $^0$c.
- Low pressure cryogenics: 28000 gal Liq. $H_2$, 13500 gal LOX , Vacuum jacket feed lines
- 11 $m^3$ gaseous oxygen at 3000 psi

## Test stand 403

It is a 9.75 m diameter by 10 m high carbon steel altitude chamber capable of accommodating a vehicle with a thrust vector controlled capable of accommodation a vehicle with a thrust vector controlled, 110 kN thrust engine firing vertically downward. T can test articles of 4.6 m by 4.6 m by 13.7 m tall. It consists of 3 interior levels which can be re configured to meet test requirements.

Specifications:

- Single position, vertical firing capability
- Altitude test capable to 30.5 km for engine firing with steam system; up yo 250 K Ft nonfiring with vacuum pumps
- Propellants: $N_2O_4$ and Hydrazine
- Propellant capability – 2000-gal storage/run tanks for hypergolic propellants can be saturated with helium up to 300 psi; both propellants can be temperature conditioned from 4 to 49 $_0$c; pressure or pump transfer of propellants; two propellant aspiration systems installed
- Maximum thrust – 111 N; vertical firing; screw-jack precision test article positioning

system; ambient pressure-temperature conditioning from -1 to 49 $^{0}$c

- Low pressure cryogenics: 28,000 gal liquid hydrogen, 13,500 gal liquid oxygen, vacuum jacketed feed lines
- 11 $m^3$ gaseous oxygen at 3000 psi
- 500-gal, 600-psi hydrocarbon fuel system (currently ethyl alcohol)

## Test stand 405

Test stand 405 is a horizontal firing stand, complete with a 2.9 m diameter by 8.5 m long altitude chamber that is capable of testing both solid propellant rocket motors up to 110 kN thrust and hypergolic engines up to 4.5 kN thrust.

Specifications:

- Horizontal firing capability
- Altitude test capability to 30.5 km for engine firing with steam system; up to 76 km non firing vacuum pumps
- Maximum thrust – 111 N; horizontal firing
- Propellants: $N_2O_4$, Hydrazines and solids
- Propellant capability – MMH/ $N_2O_4$ - 110-gal run tanks rated to 1,000 psia; both propellants can be saturated with helium up to 285 psi; both propellants can be temperature conditioned from 4 to 49 $^{0}$c.
- Solid motor capability – data acquisition ad control slip ring for motor rotation up to 120 rpm during firing; side and axial thrust measurement system

## Test stand 406

Test stand 406 is 12 Cm diameter by 2.5 m long.

Specifications:

- Maximum thrust – 4.5 kN; horizontal firing
- Altitude capability – 30.5 km for engine firing with steam system; up to 76 km non-firing with vacuum pumps

### 2.2.2 ESA[11]

One of DLR Lampoldshausen's key role is to build and operate test beds for space propulsion systems on behalf and in collaboration with the European Space Agency (ESA). DLR has built up a level of expertise in the development and operation of altitude simulation systems for upper-stage propulsion systems that is unique in Europe. The final acceptance of P4.1 HAT facility was achieved in 2010 in Germany. The task was to do special operations linked to Start-up and

shut-down of the Engine with respect to Nozzle loads. The energy of exhaust gas from running engine is used to maintain vacuum. The diffuser section compresses and decelerates the flow. Additionally steam jet ejectors and condensers maintain the necessary pressure conditions. Such large amounts of steam are produced by injecting water into rocket exhaust which then get vaporised. This steam is used in the ejectors.

Other notable features of this facility are the use of Centre body diffuser and adapters to test various test configurations on the same test position. Special attention is given to dynamic behaviour of Altitude conditions. The analysis of LOX/LH2 explosion with regard to the evacuated safety areas and constructions is ongoing. The data of failures of upper stages during the Saturn program in USA provides valuable information. For modelling, FLACS (Flame Acceleration Simulator) from the Norwegian company GEXCON is used.

Research is still going on. Driving factors are new nozzle designs with high expansion ratios, new materials like ceramics, advanced nozzles like expandable nozzles or dual bell nozzles and throttled engines with variable thrust levels require new technologies for testing close to flight conditions. An Engineering project “Advance Altitude Simulation AAS-P8” was initiated to develop and design an experimental set-up to improve the altitude simulation and to test nozzles with flight loads on a sub-scale level. A new test position p5.2 is to perform the qualification of the new upper stage with the VINCI engine.

### 2.2.3 JAXA

The Kakuda Space center (KSPC) leads research and development in rocket engines, which are the hearts of the vehicles that carry satellites into outer space. The KSPC has also played an important role in improving rocket engines. In addition to the research, development and testing of liquid-propellant engines for the H-IIA and other launch vehicles the KSPC has also been playing an important role for R&D of an apogee engine for a satellite as well as of a small spherical solid rocket motor. Various research, from basics to applications related to launch vehicle engines turbo pumps, combustors, and nozzles, is also conducted at the KSPC to contribute to improving Japan’s launch vehicle engine technology. Lately, they are also engaging in development of a compound engine as a future high-performance engine that can be used both on the Earth and in space. Experiments and research by simulating re-entry to the atmosphere are also performed at the KSPC. [12]

The simulated altitude is approximately 30 Km in this facility and its the first one made in Japan. It has been used for the development of H-I and H-II launch vehicle. The exhaust system of the facility consists of a two stage section ejector and supersonic diffusers connected to a liquid rocket engine test capsule.[13]

### Engines that can be tested

- Propulsion: 100kN (mas)
- Horizontal Stand with Gimbals
- Propellant: LOX/liquid hydogen, liquified natural gas, gaseous hydrogen and gaseous

methane

## Gas plant (charge and discharge gas)

- Discharge system: diffuser and sSection driven double-banked ejector
- Boiler pressure: 4.3MPa (saturate)
- SSection accumulater pressure: 4.2MPa
- SSection ejector pressure: 1.3MPa
- SSection volume: 1.7kg/s
- SSection generate volume: 160kg/s x 180s
- First stage sSection flow rate: 40kg/s
- Second stage sSection flow rate: 120kg/s
- Test pressure at ignition: 4kPa at Steady combustion: 1kPa (for Liquid rocket engine with 50kN of propulsion)

## 2.3 Theory of flow separation

The foremost purpose of a HAT facility is to prevent flow separation which causes structural damage to the nozzle. We know that flow separation occurs when the gas in the boundary layer is unable to negotiate with the rise in ambient pressure at the end of the nozzle. It was first suggested that separation occurs when [2]:

$$P_{exit} / P_{ambient} = 0.4$$

It was found that for short contoured nozzles:

$$P_{all} / P_{ambient} = 0.583 * (P_{ambient} / P_c)^{0.195}$$

where,

$P_{wall}$ = exhaust gas static pressure on wall at separation

$P_c$ = chamber pressure = Exhaust gas total pressure

$P_t$ = Total pressure

$P_a$ = ambient pressure

$P_e$ = exit pressure

Flow separation can be characterised as:

- Free shock separation
- Restricted shock separation

At low exit Mach numbers it is useful to use the data falling below the graph of [3]:

$$A_s / A^* = 0.8 * [(A_e / A^{*)} - 1] + 1$$

the flow will not separate for $P_t / P_a$ above this curve:

$$P_t / P_a = 1 + 0.39 * (P_t / P_e)$$

Separation can be predicted using Zero Pressure gradient free interaction theory over most of the nozzle length for wall divergence angle greater than $10^0$. Since it is not in our best interest to theoretically study separation, one may best avoid it during nozzle testing and operation. Free shock separation is not influenced by the downstream geometry. Hence correlations relating to inlet pressure also exist [14]:

$$P_s / P_a = 1.082 – 0.363\ M_s + 0.386\ M_s^2 \text{ for } M_s = 2.4 \text{ to } 4.5$$

for $Re > 10^5$ and $M_i$ between 1.4 to 6.0

$$P_s / P_i = 1 + 0.73\ (M_i / 2)$$

$$P_p / P_i = 1 + (M_i / 2)$$

For free shock separation schilling suggested:

$$P_i / P_a = a * (P_c / P_a)^{\ b}$$

where

a = 0.582 b = -0.195 contoured nozzle

a = 0.541 b = -0.136 conical nozzle

a = 2/3 b = -0.2 used by Kalt and Badl. Found to be in better agreement experimentally

Schmucker used:

$$P_i / P_a = (\ 1.88\ M_i - 1)^{-0.64}$$

It was well noted that the separation line moves towards nozzle exit as chamber pressure is increased or when ambient pressure is decreased.

## 2.4 Flow Separation in HAT

Flow separation occurs in an over-expanded supersonic rocket nozzle when the pressure at one point of the nozzle wall reaches a value which is 50 to 80 percent lower than ambient pressure. The boundary layer of a rocket engine during hot firing is mostly turbulent, only turbulent separation will be considered here [15].

Flow separation occurs when:

- Velocity at the wall is zero / Negative; and an inflection point exists in the velocity profile.
- And when a positive or adverse pressure gradient occurs in the direction of flow
- At low Reynolds numbers (Re < 1), the inertia effects are small relative to the viscous and pressure forces. In this flow regime the drag coefficient varies inversely with the Reynolds number. For example, the drag coefficient CD for a sphere is equal to 24/Re.
- At moderate Reynolds numbers (1<Re<103), the flow begins to separate in a periodic fashion in the form of Karman vortices.
- At higher Reynolds numbers (103 < Re < 105), the flow becomes fully separated. An adverse pressure gradient exists over the rear portion of the cylinder resulting in a rapid growth of the laminar boundary layer and separation.

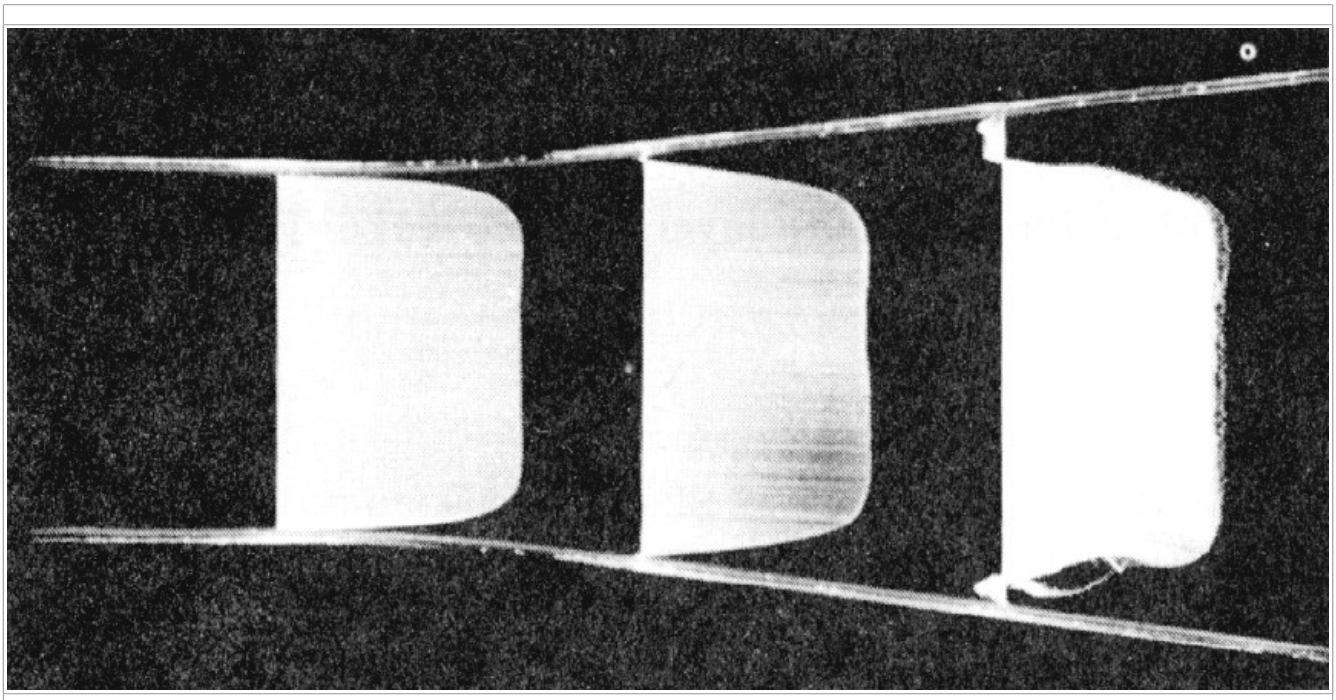

**FIgure 2-2: Flow separation in diffuser with a large angle**

- As the Reynolds number increases, the boundary layer transitions to turbulent, delaying separation and resulting in a sudden decrease in the drag coefficient

- In the case where the boundary layer is laminar, insufficient momentum exchange takes, the flow is unable to adjust to the increasing pressure and separates from the surface.
- In case where the flow is turbulent, the increased transport of momentum (due to the Reynolds stresses) from the free-stream to the wall increases the stream wise momentum in the boundary layer. This allows the flow to overcome the adverse pressure gradient. It eventually does separate nevertheless, but much further downstream.

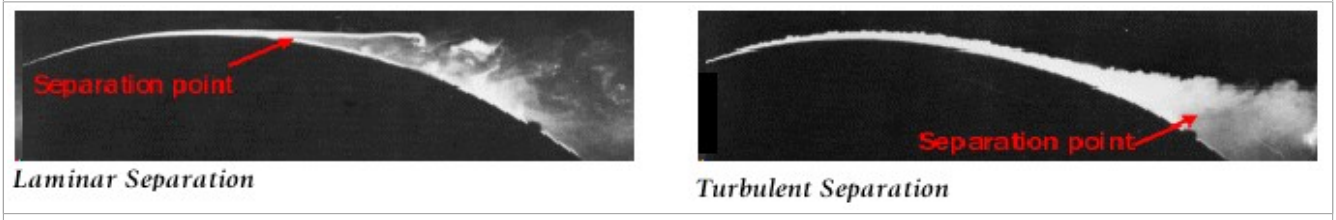


**Figure 2-3: Point of separation in laminar and turbulent flows**

Just as flow separation can be understood in terms of the combined effects of viscosity and adverse pressure gradients, separated flows can be reattached by the application of a suitable modification to the boundary conditions. In the below example, suction is applied to the leading edge of the air foil at a sharp angle of attack, removing the early separation zone, and moving the separation point much further downstream.

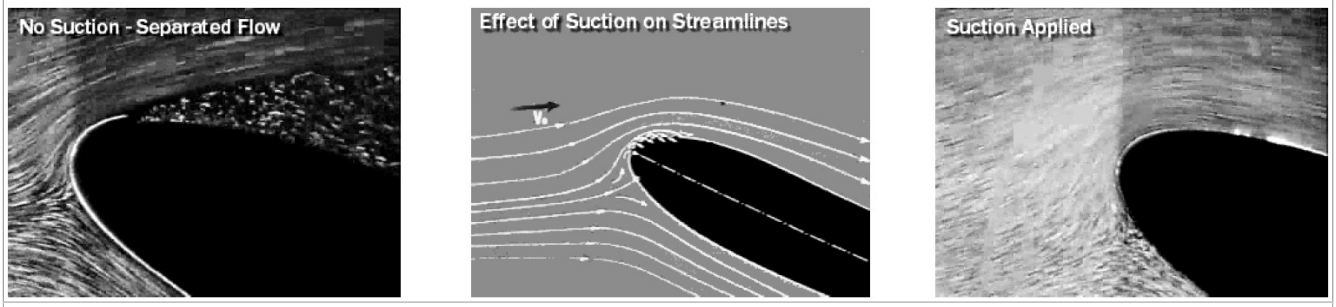


**Figure 2-4: Effect of suction on flow separation**

## 2.5 CFD Analyses

Altitude testing presents a risk of failure to both the Thrust Chamber and the apparatus being used. As it was discussed earlier, flow separation may cause unsymmetrical radial loads that can cause structural damage to the nozzle and high temperature exhaust gases may cause thermal failure of the apparatus. Therefore it is necessary to perform CFD analysis and predict the operating parameters of the test. Various mathematical models predict the performance at different accuracies and require different computational time. A resource economical and sufficiently accurate analysis is eminent.

A segregated implicit solver with the Spalart – Allamaras turbulence model was adopted to

compute the flow pattern inside the diffuser and ejector system. In many compressible flow applications, the temperature goes well beyond 3000 K. Hence the assumption of calorifically perfect gas becomes invalid [3]. In another report a fully coupled, implicit, compressible flow solver with the Spalart–Allmaras turbulence model was adopted to compute the flow pattern inside the HAT facility.

Coupling of exhaust gas and discrete droplets is difficult. In order to simplify the analysis, an equivalent approach of distributed mass sources and heat sinks in the gas phase momentum and energy equations was applied to incorporate the effect of evaporating water droplets. This simplification results in appreciable reduction of the computational time required without significantly affecting the predicted performance characteristics of the HAT facility [16].

A finite volume scheme and density-based solver with coupled scheme were applied in the computational process. RSM turbulent model, implicit formulations were used considering the accuracy and stability. Second-order upwind scheme was used for turbulent kinetic energy as well as spatial discretisation. The flow is governed by the three-dimensional, compressible, steady state/ unsteady-state form of the fluid flow conservation equations. Reynolds Averaged compressible Navier–Stokes (RANS) equations are used in this work, and they have been stated to be more suitable for variable density flows.

In one of the analysis of chevrons (a 3-D modification to the outlet of a pipe to increase the mixing of fluid from two pipes into a single pipe) it was concluded that under the chevrons influence, more longitudinal vortices were generated, more rotary stream passed through the mixing chamber and introduced more shear stress to propel the secondary stream into the vacuum ejector [17].

Once again Spalart Allmaras turbulence model was used in one of the analyses for flow simulations [18].

## 2.6 Complications involved in Analyses and Testing

The complication involved in modelling a full-scale HAT facility arises primarily due to the coupling of continuous gas phase flow with the motion of discrete phase droplets in the spray cooler. Particularly, as the Lagrangian formulation is applied to track all of the individual droplets the computational effort increases to a great extent [16]. This is especially true for J2-X that is developed by NASA. Facility designs require a complex network of diffuser ducts, steam ejector trains, fast operating valves, spray nozzles and flow diverters that need to be characterised for steady state performance. More importantly, integrated facility designs will also have to be evaluated for start-up/shut-down transients. This is because they can trigger engine non-starter modes leading to catastrophic failure [20].

The turbulent modelling of a compressible flow must be able to take into account the additional correlations that involve the fluctuating thermodynamic quantities and fluctuating dilation. It has to be borne in mind that the interaction of the shock wave with the turbulent layer would lead to a significant increase in turbulent intensity and that shear stress across shock would also increase. To take account of this important feature at high-speed flow, in one of the studies, a

combined model of the low Reynolds number k-ε model and compressible-dissipation and pressure-dilatation proposed by Sarkar was used. And also unsteady numerical analysis was performed in order to consider unsteadiness of the flow structure and oscillatory vacuum chamber pressure at minimum start-operating condition [21]. The standard k-ε model, which was proposed for high Reynolds number flows, is traditionally used with a wall function and the variable $y+$ as a damping function. However, universal wall functions do not exist in complex flows, and the damping factor cannot be applied to flows with separation. Thus, a low Reynolds number k-ε model was developed for near wall turbulence. Within certain distances from the wall, all energetic large eddies will reduce to Kolmogorov eddies (i.e. the smallest eddies in turbulence), and all the important wall parameters, such as friction velocity, viscous length scale, and mean strain rate at the wall can be characterised by the Kolmogorov micro scale [22].

There was a mention in a 1973 report compiled by a joint investigation team from the Defence Department and NASA in the United States, over a period of five to six years for development of a modern propulsion systems. It was recommended that 50,000 hours of testing should be conducted on high altitude stands, with use of three or four testing compartments. It was recommended to provide appropriate injection water in the flame extinguishing stage so that a backward propagation of an ignition source (that may remain) can be prevented. Thus damage to gas suction pipe lines can be avoided.

In one of the reports a hazard of explosion was made mention. In this particular case of the Chinese test facility, to prevent destruction of the test compartment by accidental explosion, 10 explosion windows were installed in the compartment [23].

There is some small amount of thrust “overshoot” at ignition and “blow back” with the exhaust flow breakdown at cut-off. It is essential to minimise the amount of blow back into a delicate engine nozzle and base region so as not to cause test article damage. Thus it was suggested to use all the almost all original components for the test during the test of the J-2 engine. The J-2 Engine and all propellant lines, vent and purge lines, valves, and avionics were the actual flight systems. Only the Stage had thick walls for safe ground testing [24].

# 3. Design of HAT facility

## 3.1 Configuration of the Diffuser

It was showed that the Diffuser pressure recovery of an Ejector-Diffuser system can be greatly increased when a second throat is employed. This increase is of considerable interest in the design of Ejector-Diffuser systems for Rocket test facilities. Because the increasing requirement for high altitude facilities is limited by the available cylindrical diffuser pressure recovery [25]. It was also noted that a STED (Second Throat Ejector Diffuser) system would start at a second-throat contraction considerably greater than that allowed by the wind tunnel normal shock limitation [26]. A second throat Ejector-Diffuser system can be employed to create the low pressure environment of the high altitude flight situation during the testing of large area ratio rocket motors [27].

## 3.2 The Second Throat

It was showed that when the Second throat (the throat section of the diffuser) is positioned too far up-stream relative to the facility then the jet impinges on the walls of the ramp (angled wall) causing the pressure to increase locally. On the other hand if it is too far down-stream the diffuser did not enter ‘started’ condition because of the decrease in the Mach number that is entering the second throat. Thus it was concluded that the optimum location would be such that free-jet impingement is upstream of the second-throat ramp for second throats of all lengths.

The most efficient second-throat geometry for an available diffuser length would be an intermediate length second throat with a subsonic diffuser. It was also suggested that if the second throat is located at or near its optimum position, the duct friction term will be very small. Whereas if the second throat is located considerably downstream from its optimum location, the duct friction loss may become significant [28]. For a second throat type diffuser, although the second throat contraction has a strong impact, the ramp angle does not have a significant effect on the operational characteristics [29].

## 3.3 The Diffuser section

The supersonic rocket plume is decelerated in the diffuser to recover pressure by means of a complex shock train system. In a High Altitude Test (HAT) facility, the momentum of the rocket exhaust is utilised to push the shock system beyond the divergent portion of the diffuser. It was analysed that shock structure prevailing in the diffuser system seals the vacuum chamber against ingress of atmospheric air from outside.

The location of the shock inside the diffuser depends on parameters such as:

- Chamber pressure
- Annular gap between nozzle exit and diffuser inlet

- Length of diffuser throat
- Area ratio of diffuser exit to throat
- Diffuser back pressure

During the full flow condition of the rocket motor, the exhaust plume expelled from the rocket motor at a very high speed impinged on the entry duct of the diffuser wall and caused a series of oblique shocks that terminated with a normal shock at the divergent part of the diffuser. Through this complex shock train system, the pressure is recovered in the diffuser system by decelerating the supersonic flow to subsonic flow. The terminal normal shock would be positioned inside the diffuser system depending upon the pressure recovery of the diffuser (diffuser back pressure).

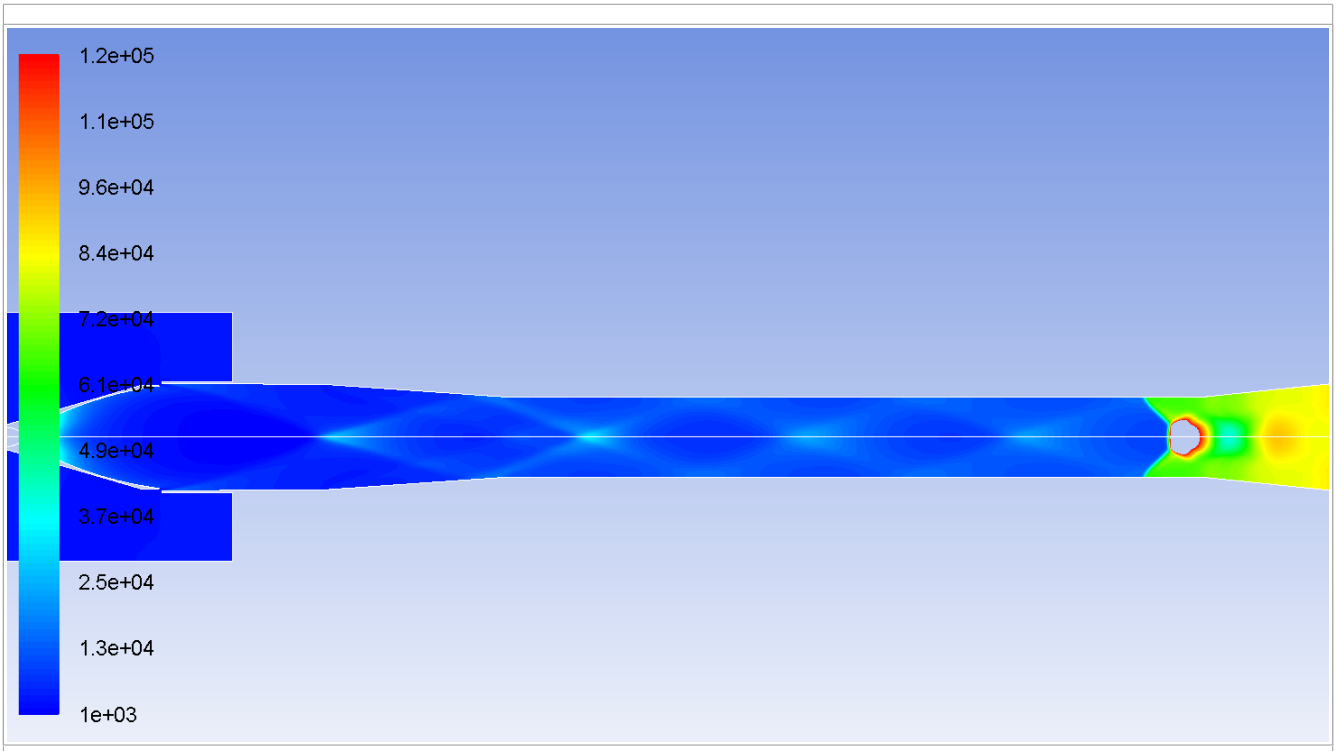


**Figure 3-1: Contours of Pressure showing Shocks in HAT**

When diffuser exit pressure is less than atmospheric pressure, an external ejector system is required to pull the flow from diffuser to the atmosphere. It was shown that during the full flow condition of the rocket motor, the momentum of the rocket exhaust is itself sufficient to maintain the low vacuum condition with the help of the shock developed in the second throat diffuser. This complex shock pattern in the diffuser system is advantageous because it seals the vacuum chamber from any back flow will spoil the low vacuum level.

The performance of the diffuser depends on the mass flow rate of the driving fluid used in the ejector. As back pressure at the diffuser exit is lowered, the prevailing shock system moves away from the rocket nozzle, thus enabling the maintenance of vacuum in the vacuum chamber [27].

It was concluded that the flow regime was not the only important factor for the diffuser performance, but also the inlet conditions affected the performance more than the flow regimes. They also presented that a best area ratio existed for each diffuser length to reach the best recovery [30]. The time period required to establish steady flow in supersonic diffusers and observed that the starting times increase with diffuser length [31].

## 3.4 Cooling requirement

As the flow is decelerated in the diffuser system, the temperature across the normal shock increases which almost equals the stagnation temperature of the rocket motor exhaust that is typically around 3500 K. Therefore, to protect the diffuser wall material from thermal failure, necessary cooling arrangement should be made. The temperature drop across the diffuser wall helps to protect the diffuser hardware [27].

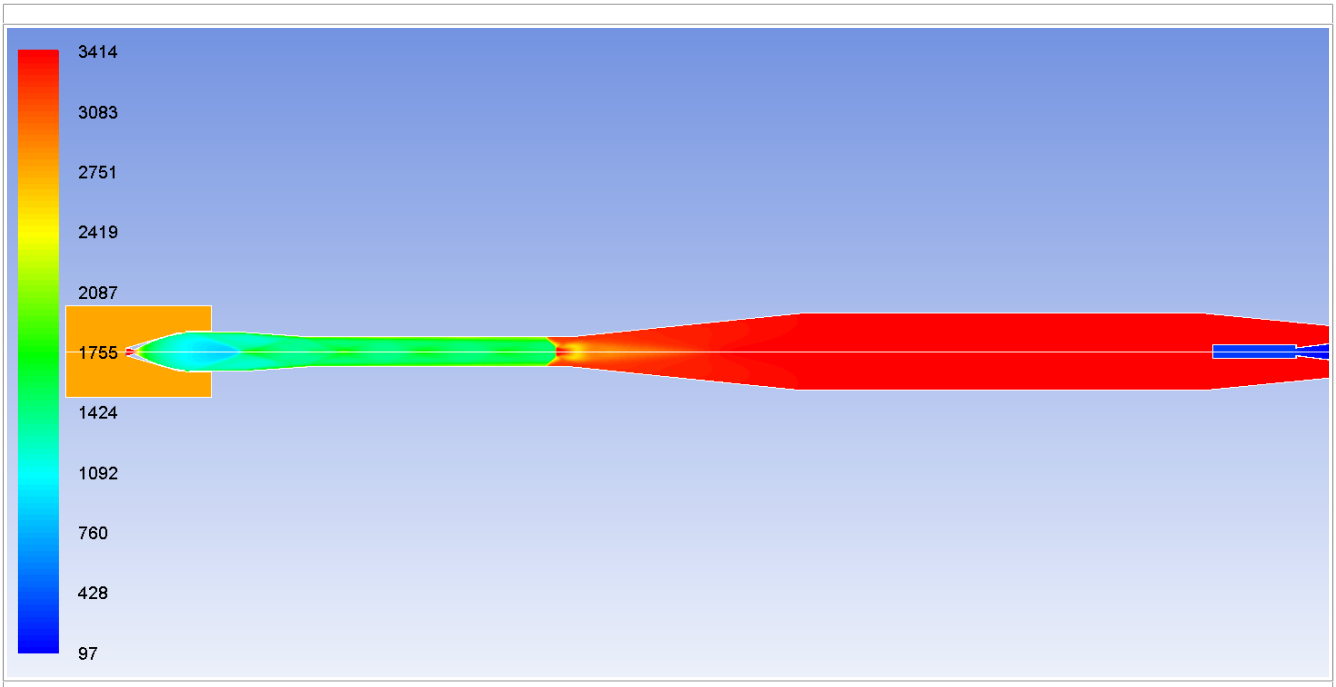


**Figure 3-2: Temperature (k) variation in HAT**

Although the addition of water in the spray cooler significantly increases the load of the ejector, the temperature drop caused by it compensates for the additional load [16].

## 3.5 The Ejector

An ejector is employed to create a low pressure environment of the flight situation to start the rocket motor effectively. It was shown that for a given mixer throat diameter of the ejector, there

exists an optimum nitrogen mass flow rate which can be determined, for pre-evacuating the vacuum chamber and ensure smooth starting of the rocket motor during the ignition phase. It was observed that for a fully started motor, the ejector fluid mass flow rate could be reduced or even made zero, due to the self-pumping action of the rocket motor exhaust as it flows through the diffuser [27].

During the initial starting phase of the rocket motor, enormous quantity of primary fluid (usually air or nitrogen) is required in the ejector system to pull the shock out of the engine, so as to maintain the low vacuum level inside the vacuum chamber [30]. It was analysed that optimum performance of an ejector can be achieved if the primary flow expanding from the ejector nozzle just fills the entire duct of the mixer throat in a smooth manner; the presence of a small annular gap or a strong impact of jet on the duct wall can lead to deterioration in the performance of the ejector [32].

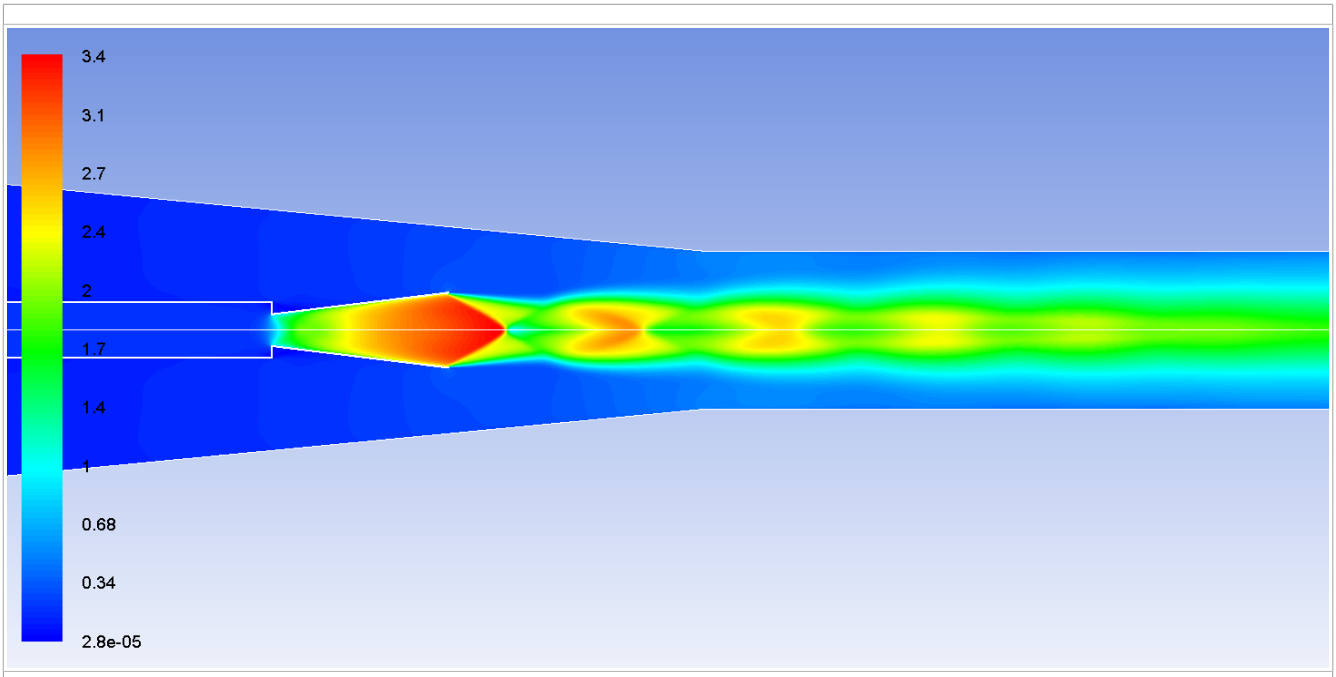


**Figure 3-3: Mach contours showing annular gap during Ejector start up**

When the nitrogen jet expanding from the nozzle just attaches to the duct walls smoothly without any gap then the complete momentum of the jet can be utilised to evacuate the test facility. On the other hand, for fluid flow rates higher than the critical value, there is a strong impact of the jet on the duct walls. At this condition, some of the jet momentum was wasted due to the impact on the wall, because of which the vacuum chamber pressure increased slightly.

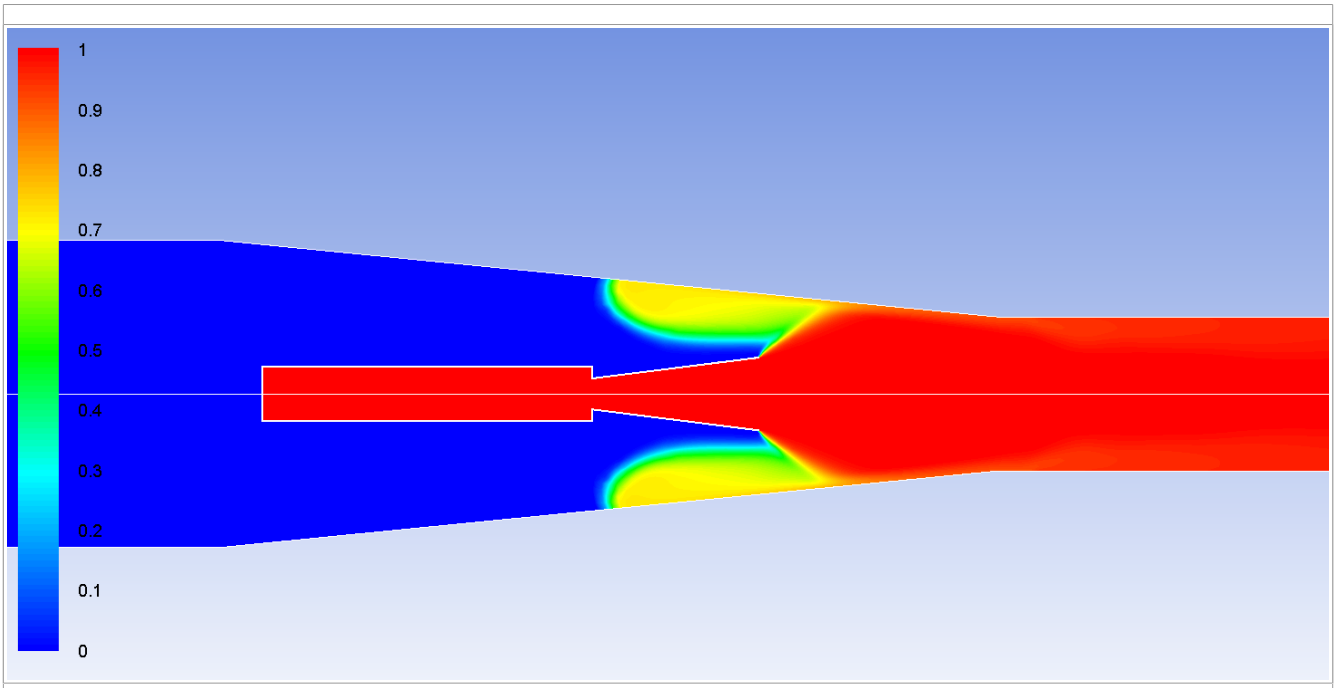


**Figure 3-4: Mole fractions of Nitrogen showing strong impact**

Because the engine exhaust is cooled with a water spray, the ejector should have adequate capacity to pump out the evaporated water mass. In other words, the ejector should be able to successfully eject the rocket exhaust gas and coolant vapour into the atmosphere at part load or full load conditions of the rocket motor, while maintaining the favourable low vacuum level in the test chamber for realising the vacuum thrust of the engine [4].

# 4. Analysis

## 4.1 Governing Equations

Any CFD simulation involves solving a set of equations (like the continuity, momentum, energy equations) using numerical approximation. Broadly speaking there are 3 techniques of numerical discretisation and solving. They are:

- Finite Difference Method (FDM)
- Finite Element Method (FEM)
- Finite Volume Method (FVM)

For the following simulations done as a part of this report, ANSYS Fluent has been used. This commercial package uses FVM.

In this technique the computational domain is discretised into finite sized cells. Then the fluid flow properties of each cell are coupled with numerical approximation equations, which form the governing equations of the analysis. These equations are solved in iterations to give an approximate solution. So this convergence of approximate solution with actual solution is measured in terms of residuals between consecutive iterations.

The coupling of properties of fluid with numerical equations makes it easy to understand the governing equations formed from them. This is one of the primary attractions of FVM. The governing equations are:

- Conservation of Mass
- Conservation of Momentum
- Conservation of Energy

The following equations utilise an operator $\nabla$ which can be referred to as Del or Nabla or Grad. The mathematical convention dictate the following

In Carteisan Co-ordinate system Nabla is defined as:

$$\nabla = \frac{\partial}{\partial x}\vec{i} + \frac{\partial}{\partial y}\vec{j} + \frac{\partial}{\partial z}\vec{k}$$

The Gradient of a scalar is

$$grad\, p = \nabla p = \frac{\partial p}{\partial x}\vec{i} + \frac{\partial p}{\partial y}\vec{j} + \frac{\partial p}{\partial z}\vec{k}$$

The Gradient of a vector is

$$grad(\vec{v}) = \nabla(\vec{v}) = \left(\frac{\partial}{\partial x}\vec{i} + \frac{\partial}{\partial y}\vec{j} + \frac{\partial}{\partial z}\vec{k}\right)\left(v_x\vec{i} + v_y\vec{j} + v_z\vec{k}\right)$$

The Divergence of a vector is

$$\nabla . \vec{v} = \frac{\partial v_x}{\partial x} + \frac{\partial v_y}{\partial y} + \frac{\partial v_z}{\partial z}$$

The Laplacian is $\nabla . \nabla$

### 4.1.1 Conservation of mass:

This can be written as the rate of increase of mass in a fluid element is equal to the net rate of mass flowing inside the fluid element.

This gives us:

$$\frac{\partial \rho}{\partial t} + \nabla . (\rho \vec{u}) = 0$$

The first term is rate of change of density in time and the second term for net flow of mass out of the element and is called 'convective term'.

If we consider a user defined source or addition of mass from phase change then it becomes

$$\frac{\partial \rho}{\partial t} + \nabla . (\rho \vec{u}) = S_m$$

For 2-D axi-symmetric geometry the continuity is given by

$$\frac{\partial \rho}{\partial t} + \frac{\partial}{\partial x}(\rho v_x) + \frac{\partial}{\partial r}(\rho v_r) + \frac{\rho v_r}{r} = S_m$$

### 4.1.2 Conservation of Momentum

This can be written as the rate of change of momentum in a fluid particle is equal to sum of forces on it. The x component of momentum equation is given by

$$\rho \frac{Du}{Dt} = \frac{\partial}{\partial x}(-p + \tau_{xx}) + \frac{\partial \tau_{yx}}{\partial y} + \frac{\partial \tau_{zx}}{\partial z} + S_{mx}$$

The y component of momentum equation is

$$\rho \frac{Dv}{Dt} = \frac{\partial}{\partial y}(-p + \tau_{yy}) + \frac{\partial \tau_{xy}}{\partial x} + \frac{\partial \tau_{zy}}{\partial z} + S_{my}$$

The z component of momentum equation is

$$\rho \frac{Du}{Dt} = \frac{\partial}{\partial z}(-p + \tau_{zz}) + \frac{\partial \tau_{xz}}{\partial x} + \frac{\partial \tau_{yz}}{\partial y} + S_{mz}$$

where

$$\tau_{xx} = 2\mu \frac{\partial u}{\partial x} + \lambda(\nabla . \vec{u}) \qquad \tau_{yy} = 2\mu \frac{\partial v}{\partial y} + \lambda(\nabla . \vec{u})$$

$$\tau_{zz} = 2\mu \frac{\partial w}{\partial z} + \lambda(\nabla . \vec{u})$$

$$\tau_{xy}=\tau_{yx}=\mu\left(\frac{\partial u}{\partial y}+\frac{\partial v}{\partial x}\right) \qquad \tau_{xz}=\tau_{zx}=\mu\left(\frac{\partial u}{\partial z}+\frac{\partial w}{\partial x}\right)$$

$$\tau_{zy}=\tau_{yz}=\mu\left(\frac{\partial v}{\partial z}+\frac{\partial w}{\partial y}\right)$$

The sign associates with pressure is opposite to that of viscous stress (a shear stress) because by sign convention a tensile stress is taken to be positive and pressure (a normal stress) is compressive in nature.

For 2-D axi-symmetric geometries the momentum equation in x direction is

$$\frac{\partial(\rho v_x)}{\partial t}+\frac{1}{r}\frac{\partial}{\partial x}(r\rho v_x v_x)+\frac{1}{r}\frac{\partial}{\partial r}(r\rho v_r v_x)=\frac{-\partial p}{\partial x}+\frac{1}{r}\frac{\partial}{\partial x}[r\mu(2\frac{\partial v_x}{\partial x}-\frac{2}{3}(\nabla.\vec{v}))]+\frac{1}{r}\frac{\partial}{\partial r}[r\mu(\frac{\partial v_x}{\partial r}+\frac{\partial v_r}{\partial x})]+F_x$$

and in r direction is

$$\frac{\partial(\rho v_r)}{\partial t}+\frac{1}{r}\frac{\partial}{\partial x}(r\rho v_x v_r)+\frac{1}{r}\frac{\partial}{\partial r}(r\rho v_r v_r)=\frac{-\partial p}{\partial r}+\frac{1}{r}\frac{\partial}{\partial r}[r\mu(2\frac{\partial v_r}{\partial r}-\frac{2}{3}(\nabla.\vec{v}))]+\frac{1}{r}\frac{\partial}{\partial x}[r\mu(\frac{\partial v_r}{\partial x}+\frac{\partial v_x}{\partial r})]$$

$$-2\mu\frac{v_r}{r^2}+\frac{2}{3}\frac{\mu}{r}(\nabla.\vec{v})+\rho\frac{v_z^2}{r}+F_r$$

In Polar Co-ordinate system

$$\nabla.(\vec{v})=\frac{\partial v_x}{\partial x}+\frac{\partial v_r}{\partial r}+\frac{v_r}{r}$$

### 4.1.3 Conservation of Energy

The energy equation is derived from the First law of Thermodynamics stating that rate of change of energy of a fluid particle is equal to rate of heat addition to the fluid particle plus the rate of work done on it.

In a 3-D Cartesian system it is given as

$$\rho\frac{DE}{Dt}=-\nabla.(p\vec{u})+\frac{\partial(u\tau_{xx})}{\partial x}+\frac{\partial(u\tau_{yx})}{\partial y}+\frac{\partial(u\tau_{zx})}{\partial z}+\frac{\partial(v\tau_{xy})}{\partial x}+\frac{\partial(v\tau_{yy})}{\partial y}+\frac{\partial(v\tau_{zy})}{\partial z}+\frac{\partial(w\tau_{xz})}{\partial x}+\frac{\partial(w\tau_{yz})}{\partial y}$$

$$\frac{\partial(w\tau_{zz})}{\partial z}+\nabla.(k\nabla T)+S_E$$

For an incompressible flow, the mass and momentum equations can be solved together and the energy equation is solved only if there is heat transfer. But for compressible flows they are linked by the variation of density. This is possible through equation of state.

$$P=\rho RT$$

### 4.1.4 Navier-Stokes Equation

When the fluid is assumed to be Newtonian, i.e., where the viscous stress is proportional to rate of deformation then the momentum equation can be further simplified to compute. This

equation was developed by two scientists Navier and Stokes independently and is thus named after them. The Navier-Stokes equation in the form used in FVM is

$$\rho\frac{Du}{Dt}=\frac{-\partial p}{\partial x}+\nabla.(\mu\nabla v)+S_{Mx}$$

$$\rho\frac{Dv}{Dt}=\frac{-\partial p}{\partial y}+\nabla.(\mu\nabla v)+S_{My}$$

$$\rho\frac{Dw}{Dt}=\frac{-\partial p}{\partial z}+\nabla.(\mu\nabla v)+S_{Mz}$$

And if the same Newtonian model is used in the energy equation it yields

$$\rho\frac{Di}{Dt}=-p\nabla.u+\nabla.(k\nabla T)+\Phi+S_i$$

where

$$\Phi=\mu[2((\frac{\partial u}{\partial x})^2+(\frac{\partial v}{\partial y})^2+(\frac{\partial w}{\partial z})^2)+(\frac{\partial u}{\partial y}+\frac{\partial v}{\partial x})^2+(\frac{\partial u}{\partial z}+\frac{\partial w}{\partial x})^2+(\frac{\partial v}{\partial z}+\frac{\partial w}{\partial y})^2]+\lambda(\nabla.u)^2$$

This Dissipation term is always positive because it contains squared terms. This indicates that the deformation work is converted to internal energy or heat and is positive.

### 4.1.5 Turbulence modelling

The SST (Shear Stress Transport) k-ω model blends the robust and accurate formulation of k-ω model in the near wall region with the free stream independence of k-ε model in the far field. The transport equations are

$$\frac{\partial}{\partial t}(\rho k)+\frac{\partial}{\partial x_i}(\rho k u_i)=\frac{\partial}{\partial x_j}(\Gamma_k\frac{\partial k}{\partial x_j})+\tilde{G}_k-Y_k+S_k$$

and

$$\frac{\partial}{\partial t}(\rho\omega)+\frac{\partial}{\partial x_i}(\rho\omega u_i)=\frac{\partial}{\partial x_j}(\Gamma_\omega\frac{\partial\omega}{\partial x_j})+G_\omega-Y_\omega+D_\omega+S_\omega$$

where

$\Gamma_k=\mu+\frac{\mu_t}{\sigma_k}$ $\Gamma_\omega=\mu+\frac{\mu_t}{\sigma_\omega}$ where $\sigma_k$ and $\sigma_\omega$ are Turbulent Prandtl numbers for k and ω

$\mu_t=\frac{\rho k}{\mu}\frac{1}{max[\frac{1}{\alpha},\frac{SF_2}{a_1\omega}]}$ F is the blending function, S is the modulus of mean of rate of strain tensor

$\tilde{G}_k=min(G_k,10\rho\beta k\omega)$ where $G_k=\mu_t S^2$

$G_\omega=\frac{a}{\nu_t}\tilde{G}_k$

$Y_k = \rho \beta k \omega$ and $Y_\omega = \rho \beta \omega^2$

$$D_\omega = 2(1-F_1)\rho \frac{1}{\omega \sigma_{\omega,2}} \frac{\partial k}{\partial x_j} \frac{\partial \omega}{\partial x_j}$$

### 4.1.6 Boundary Conditions

The boundary conditions may belong to one of the three categories

- Dirichlet, where value of the flow variable is specified
- Neumann, where flux or gradient is specified to the flow variable
- Mixed, where a linear combination of Dirichlet and Neumann condition is specified

**Inlet Condition:** Commonly a reference pressure is specified to fix the absolute pressure at the inlet nodes. This helps set pressure corrections to zero at these nodes. Once the reference pressure is set, the absolute pressure field can be calculated. For calculating Turbulent Kinetic energy and Dissipation rates approximate formulae can be used. Typically Turbulent intensity is specified between 1% to 10%

Stagnation pressure (in case of pressure inlet) or Stagnation Temperature (in case of mass flow inlet) are also specified.

**Outlet Condition:** Usually at places where there is no change in the direction of flow and where flow is fully developed, the outlet boundary condition is specified. That is why an additional domain is considered in this case where the flow is almost perpendicular to the outlet. Here back flow turbulent intensity is specified (in case there is a back flow this value will be used, otherwise ignored) along with stagnation temperature and Stagnation pressure.

**Wall Condition:** Here no-slip condition for velocity (normal velocity to the wall = 0) and adiabatic condition is used. For both laminar and turbulent flow, the boundary layer is usually considered to be laminar. This is because the $y^+$ values that are computed are low because of inflation (meshing technique where more nodes are placed close to the wall up to a certain distance without changing the mesh in free stream)

**Axis Condition:** It implies no flow across the boundary and no scalar flux across boundary. During implementation normal velocities are set to zero (like in a wall) and the values of variables at nodes near to this boundary are set to the values next to that layer of nodes. This is similar to the Symmetry Condition only that it is applied in Polar Co-ordinate system.

## 4.2 Grid Independence

Convergence is a property which shows how close a numerical solution is to the exact solution. It is measured in terms of residuals between consecutive iterations. We know that a numerical solution matches with exact solution when the size of cells tend towards zero. Therefore

it is necessary for the size of the cells to be very small for accurate results. Even then the accuracy is lost because of round-off errors in each iteration. Moreover small cell size yield more amount of cells that require a lot of computational time and resources. Hence the cell size should be moderate in size without much compromise in the accuracy of solution.

In order to prove grid independence the following cases have been considered:

- Case 1: Mass flow rate of Nitrogen is 340 kg/s at Ejector inlet and Pressure inlet of Steam is 56.4 bar at Nozzle inlet and pressure outlet of air is 1 bar. Solved with pressure based solver
- Case 2: Mass flow rate of Nitrogen is 340 kg/s at Ejector inlet and Pressure inlet of Steam is 56.4 bar at Nozzle inlet and pressure outlet of air is 1 bar. Solved with Density based solver

From case 1:

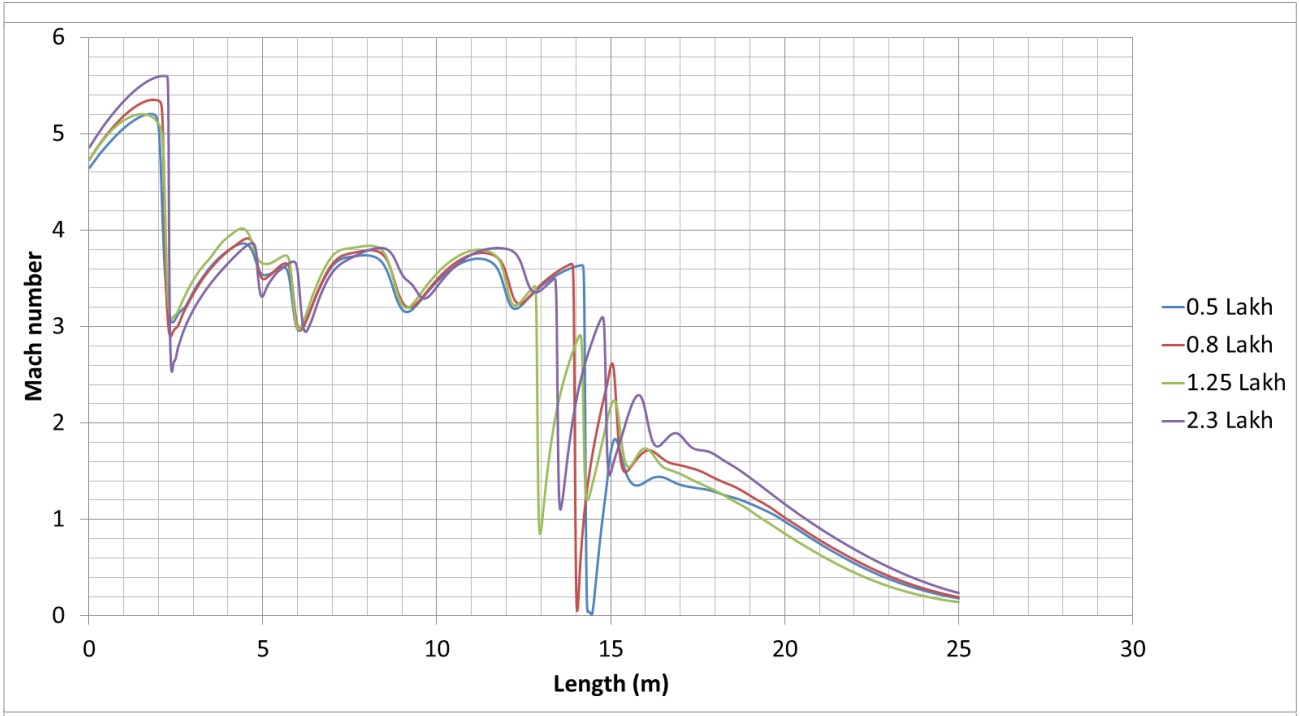


**Graph 4-1: Grid independence with Pressure based solver**

The above graph is drawn on the axis of the facility from the exit plane of the Nozzle to the end of Diffuser section. From the above graph, it can be observed that there is a slight deviation in the performance of diffuser. This can be seen in between 13- 15 m from the exit plane of the Nozzle. 0.5 and 0.8 lakh mesh indicate that the flow will drop to Mach '0' after giving a normal shock. On the other hand, 1.25 lakh and 2.3 lakh mesh indicate that the Mach will drop only to '1'. Therefore for the sake of accuracy it is recommended to use a mesh equal to or above 1.25 lakhs.

From Case 2:

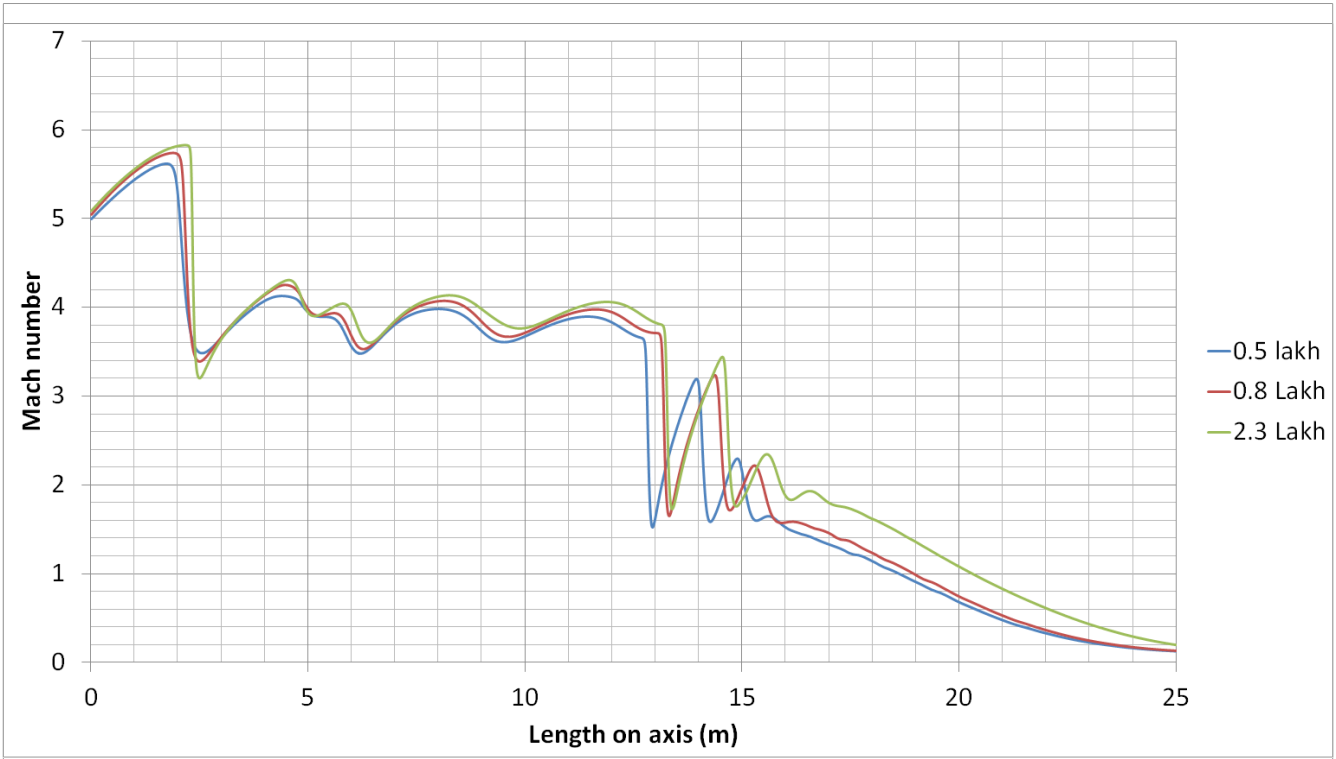


**Graph 4-2: Grid independence with Density based solver**

From the above graph, it is clear that all mesh show the same result. They also confirm with those of Pressure based solver. So any mesh can be used. It is recommended to use 0.5 lakh mesh as it matches to a greater extent with 2.3 lakh mesh. It also has the added advantage of being swift.

Flow evolution takes place more quickly with Pressure based solver, when a mass flow inlet is used. By default all equations in this solver are first order equations and hence are swift to solve. But in case of flow separation and reattachment of flow, density based solver is superior as discussed in section 4-7. Therefore in cases with flow separation, a density based solver with 0.5 lakh mesh is used and in all other cases pressure based solver with 1.25 lakh mesh is used.

The Nozzle, the Ejector and the rest of the facility are meshed as a single part to prevent mesh interfacing as shown in figure 4-3. Thin boundaries are cut inside wherever the mesh of the Nozzle or the Ejector overlap with the facility. Strong flow do not exist in the vacuum chamber. Hence the boundaries of Nozzle and Vacuum chamber differ in geometry to certain degree in order to ease meshing as shown in figure 4-4. On the other hand strong flow exist at the Ejector. Therefore care has been taken to cut a wall of very small thickness without any variation in its geometry as shown in the figure 4-5.

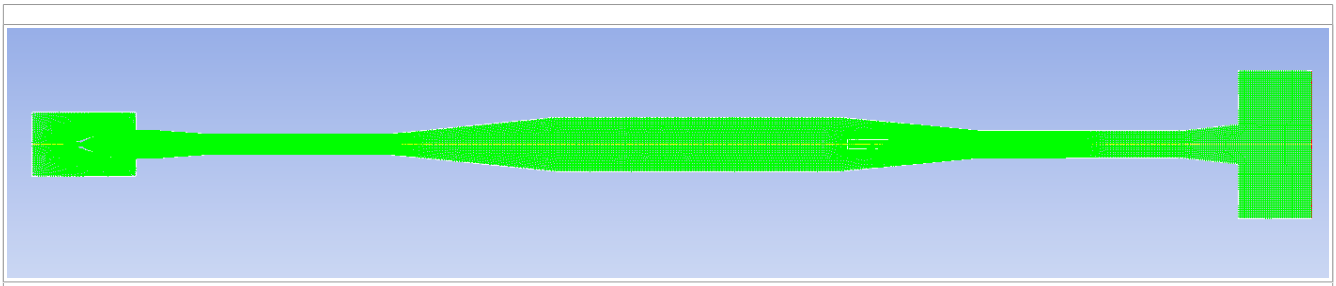

**Figure 4-3: Overall mesh**

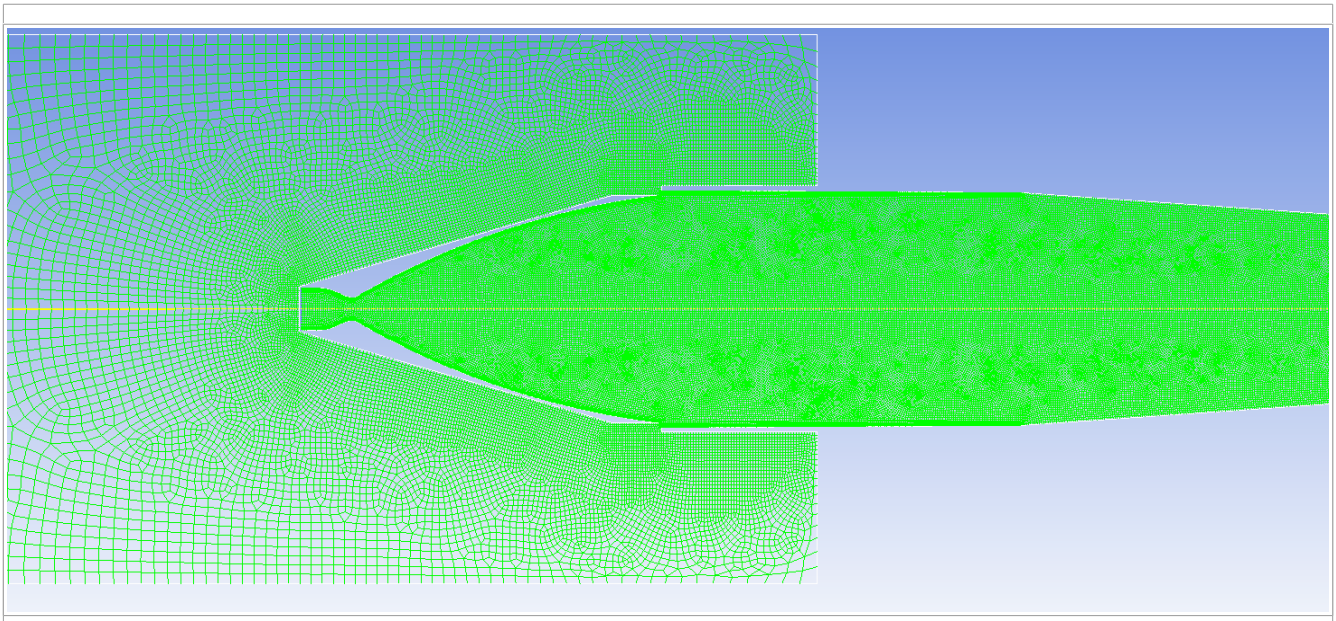

**Figure 4-4: Mesh at the Nozzle**

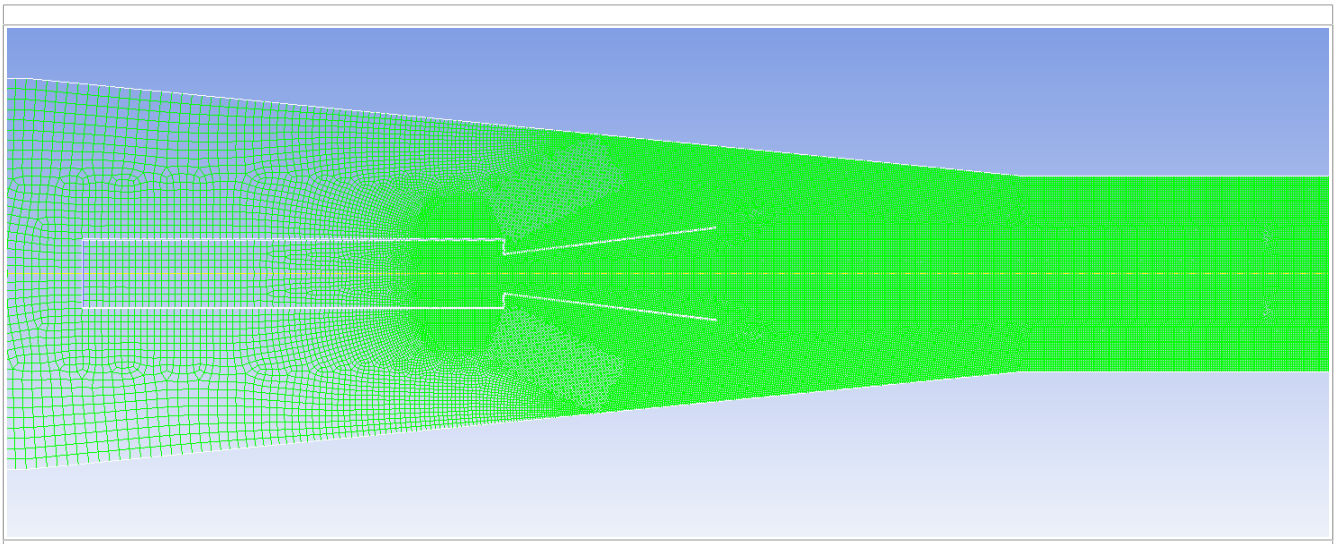

**Figure 4-5: Mesh at the Ejector**

The outlet domain is also justifiable because air (that is present at the outlet) fills up the domain during analysis and the flow is mostly perpendicular to the outlet as shown in the figure 4-6.

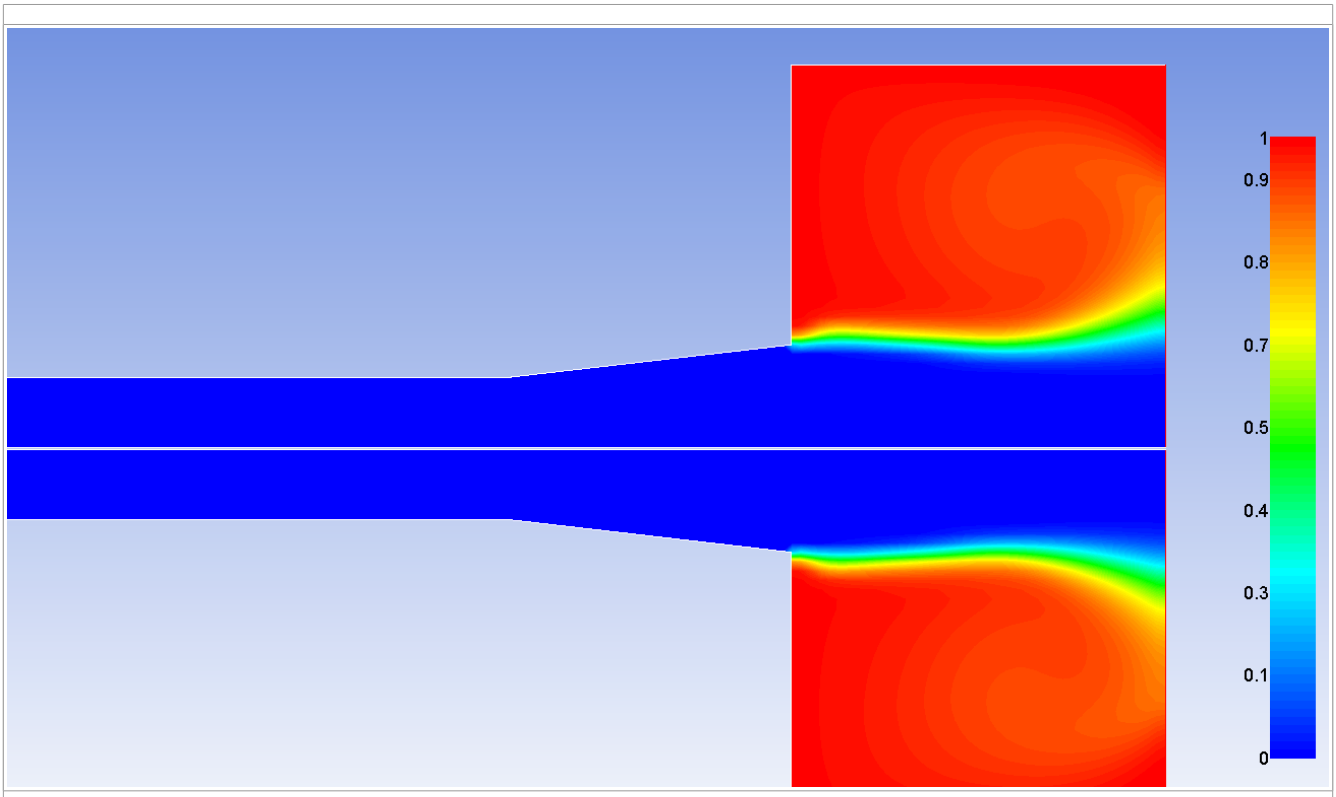


**Figure 4-6: Mole fraction of air during analysis**

## 4.3 Turbulence Model Selection

To start with, a simpler case where there is no flow separation was considered. The inlet condition at Nozzle is 60 bar and outlet is 0.1 bar pressure outlet. Various modes of Spallart-Allmaras, k-ε and k-ω were considered. All the mathematical models yielded the same results. Computational time for SA (Spallart-Allmaras) is the minimum when compared to other turbulence models because it solves only one equation where as the other two models solve two equations each.

As seen from the graph 4-7 below, the Mach number on the exit plane of the Nozzle is approximately constant until it reaches the wall. There the Mach number rapidly decreases showing the behaviour of boundary layer.

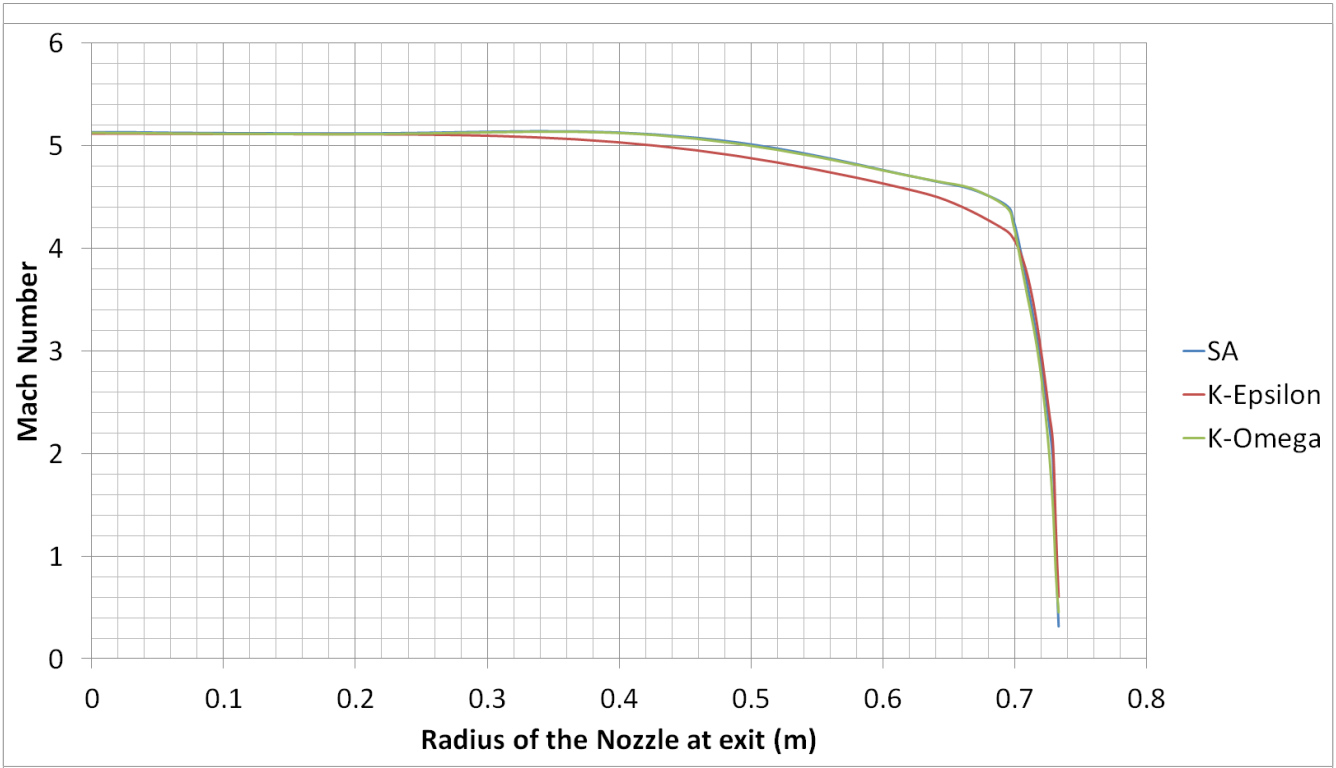


**Graph 4-7: Mach number vs Radius at outlet for 0.1 bar**

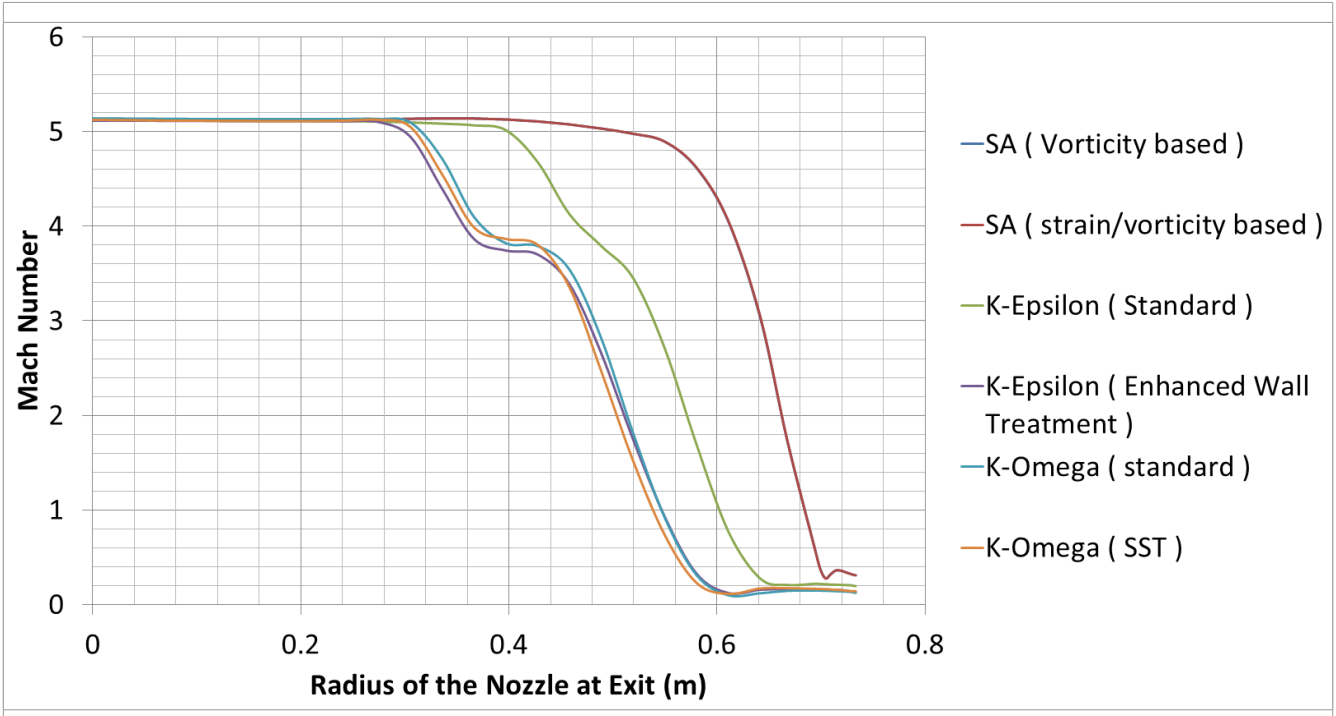


**Graph 4-8: Mach number vs Radius at outlet for 0.4 bar**

But in case of flow separation, where the pressure outlet was increased to 0.4 bar while

maintaining all other parameters the same, the results were different. From the graph 4-8, k-ω and k-ε (enhanced wall treatment) show agreeable results. We know that the purpose of HAT facility is to avoid flow separation. Therefore to find out the cases where flow separation may occur, it becomes necessary to use the k-ω SST model. Therefore the K-ω SST (Shear Stress Transport) has been used in all the remaining analyses because of its greater accuracy to predict turbulence due to introduction of additional transport equations. [33]

## 4.4 Effect of Back pressure on Flow separation

As mentioned earlier the nozzle suffers flow separation at higher back pressures. The Ejector has to be designed to maintain a pressure less than this value. Hence to find out a suitable back pressure for this nozzle an analysis was performed. The inlet pressure is kept constant at 60 bar and the outlet pressure is varied from 0.01 bar to 0.4 bar.

From the graph 4-9 we can see that flow separation starts at 0.2 bar but its is negligible. It becomes more pronounced at 0.3 bar. Therefore it is clear that pressure less than 0.2 bar is to be maintained inside the HAT facility.

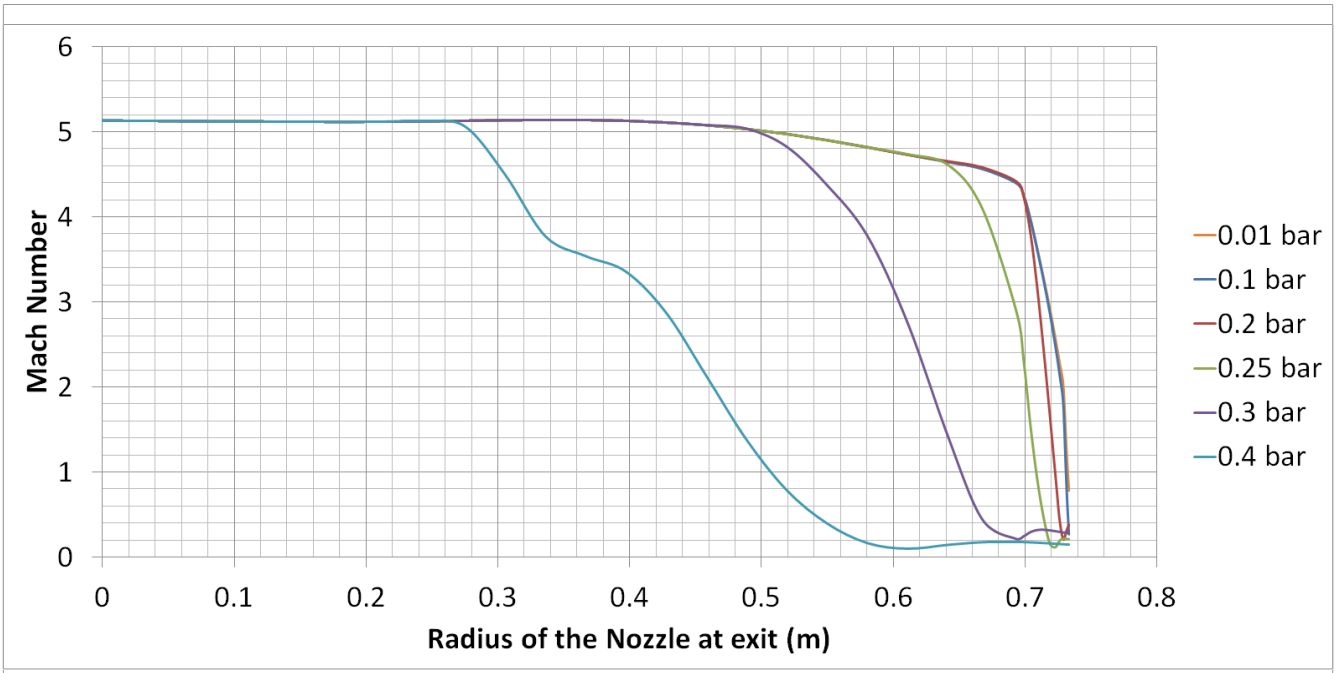


**Graph 4-9: Mach number vs Radius at outlet for varying back pressures**

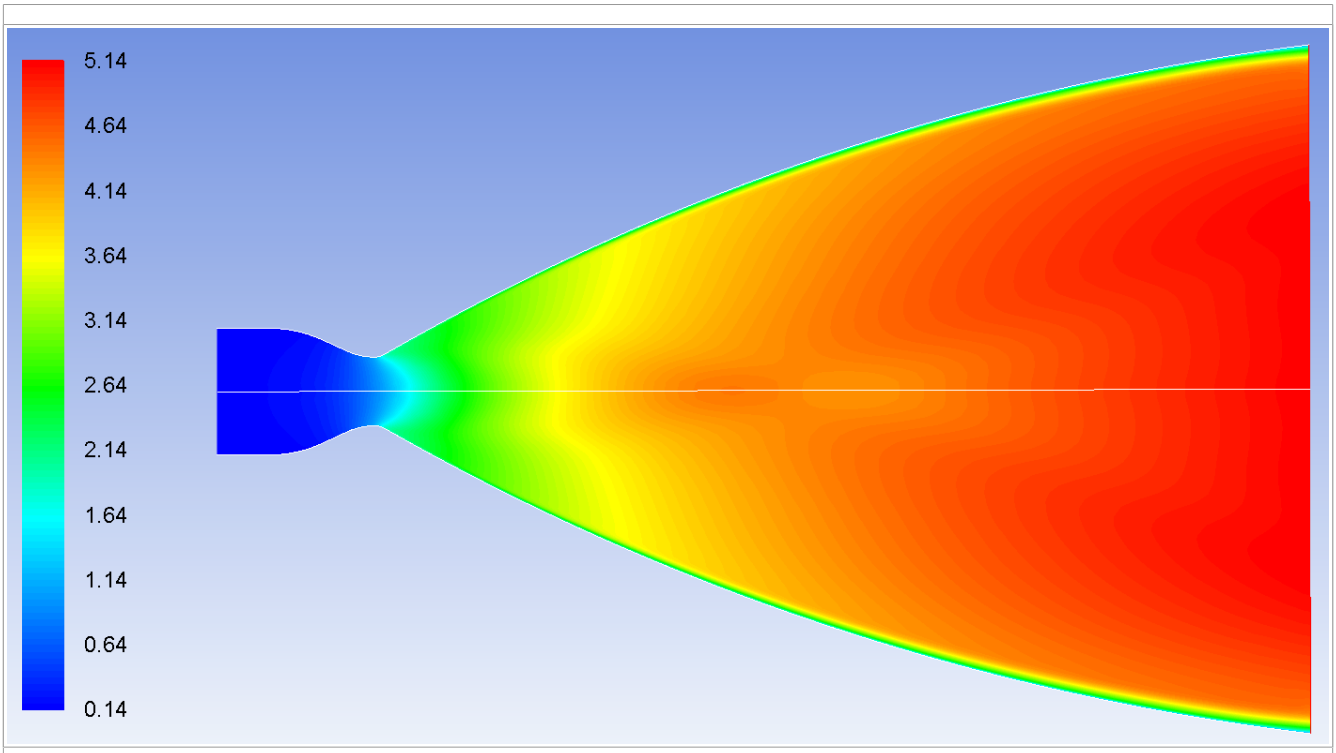


**Figure 4-10: Full flow of Nozzle at 0.1 bar**

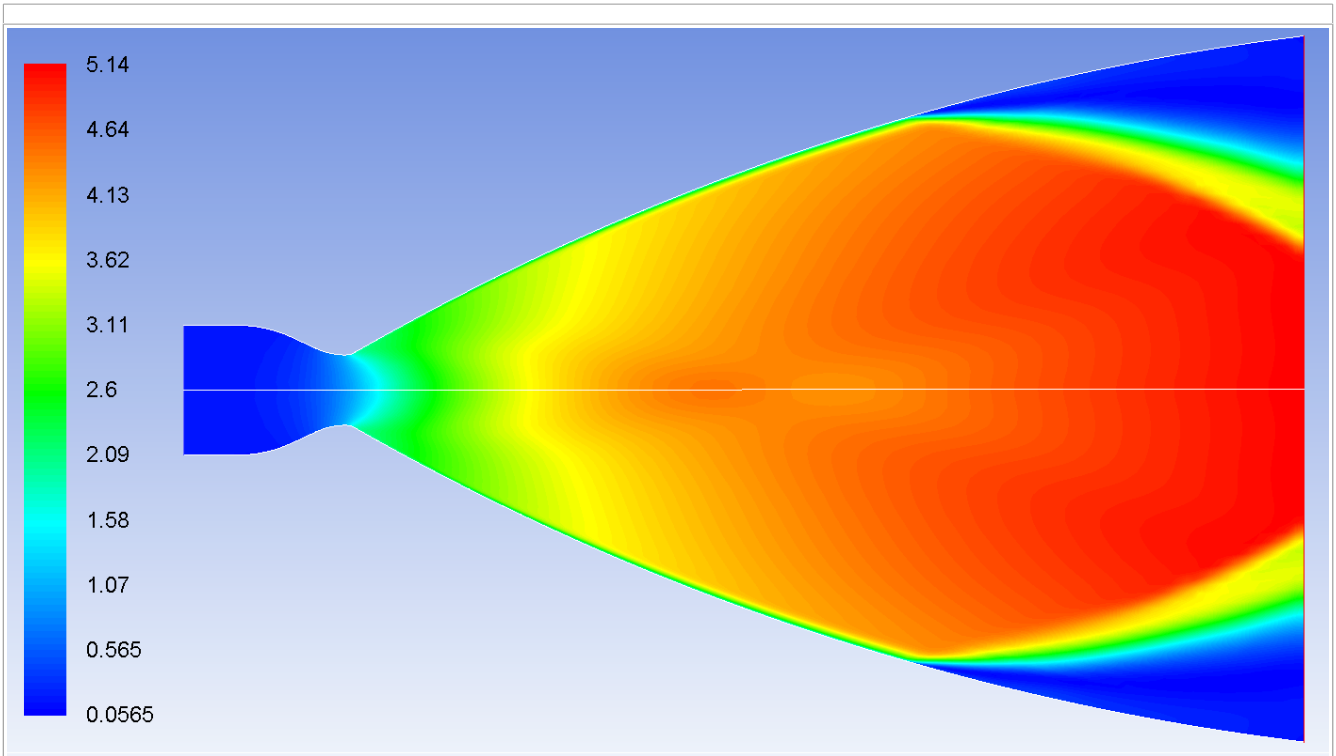


**Figure 4-11: Flow separation of Nozzle at 0.4 bar**

If we compare the two figures 4-10 and 4-11, then it is evident that during flow separation part of the Nozzle is wasted as it does not expand the flow. This leads to generation of low thrust. Due to flow separation there will be side loads on the Thrust chamber and vibration levels will also be higher. In order to prevent flow separation a pressure less than 0.2 bar in the vacuum chamber, has to be maintained by the Ejector system.

## 4.5 Ejector fluid and its optimisation

Essentially, the Ejector pumps high momentum gas through an Ejector that entrains the surrounding molecules into the flow. This flow then exits the facility and mixes into the atmosphere. Analysis has been done to choose an optimum fluid for the ejector. The graph 4-12 shows the affinity of various gases to create vacuum. The analysis was done at mass flow rate of 200 Kg/s.

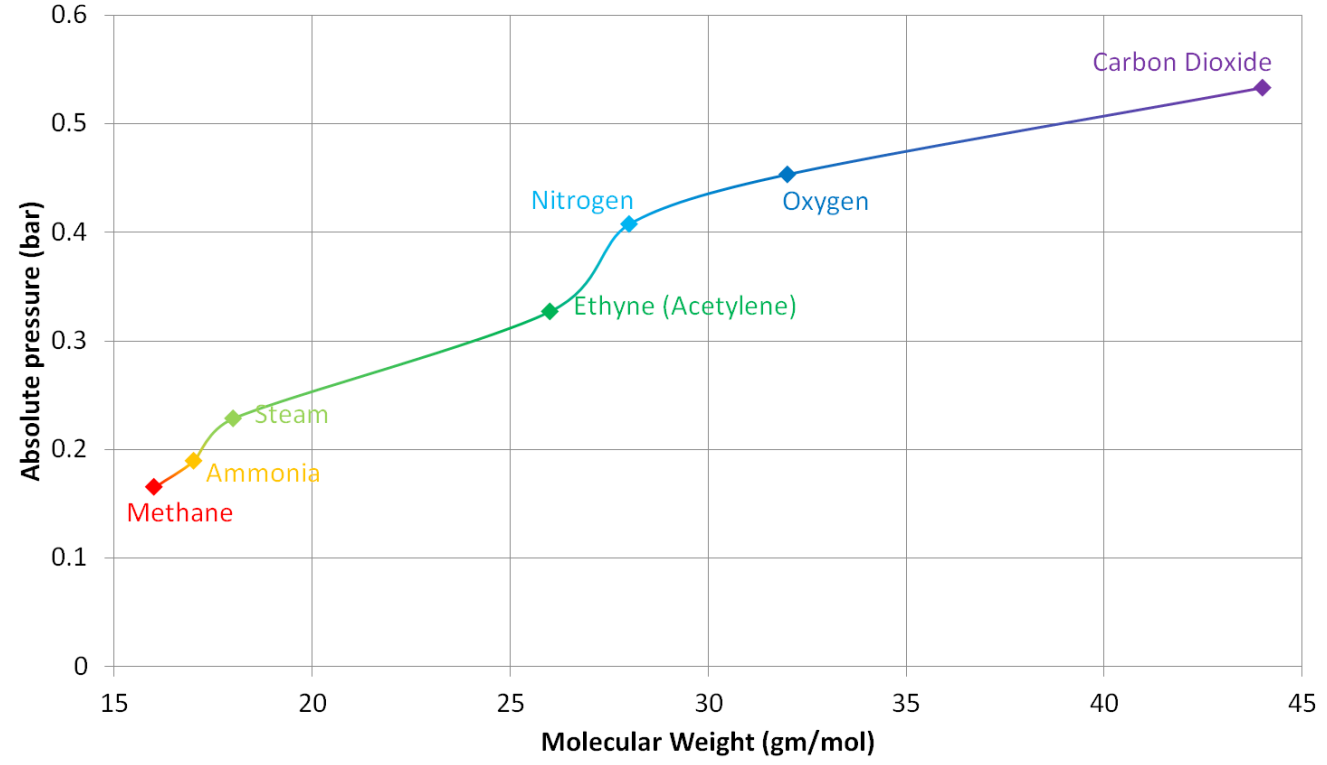


**Graph 4-12: Pressure in the Vacuum chamber for various gases**

The following observation has been made from the analyses:

- The line shows that if the molecular weight decreases then generally the pressure also decreases in the vacuum chamber
- Keeping in view the environmental considerations, cost of manufacturing, ease of handling and abundance of availability, steam is the suitable gas (even if Methane is the best gas).

So, by altering the mass flow rate we can find the optimum flow of steam required which is 270

Kg/s from the graph 4-13.

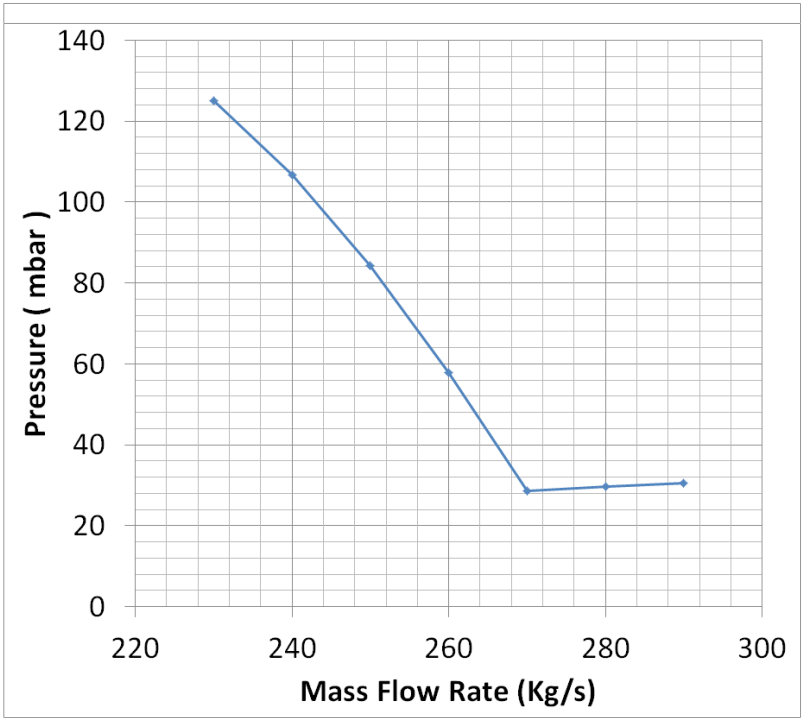


**Graph 4-13: Pressure vs mass flow rate for steam**

However, in ISRO, Nitrogen is used as the ejector fluid. Hence Nitrogen flow rate has also been optimised. Analysis results indicate that 340 kg/s is the optimum Nitrogen flow rate required for the ejector as shown in graph 4-14.

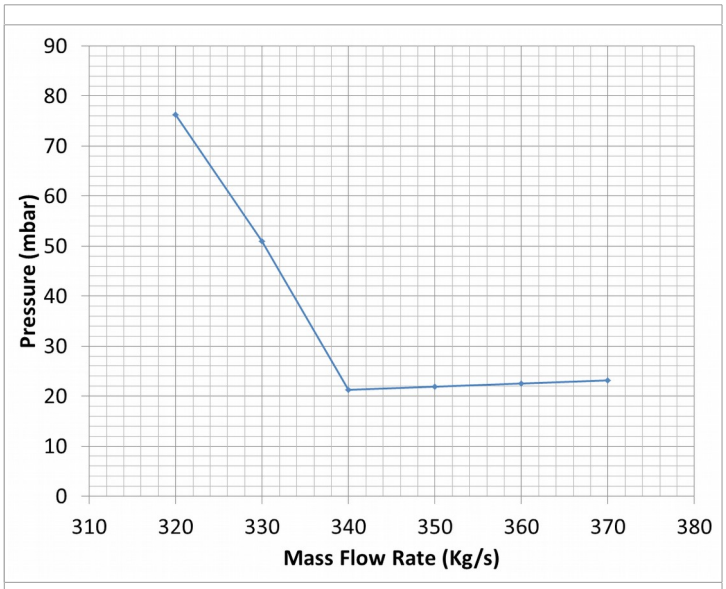


**Graph 4-14: Pressure vs mass flow rate for Nitrogen**

## 4.6 Ejector start-up

When the ejector is just started, the pressure in the Ejector-Diffuser section is still at ambient pressure which is taken as 1 bar here. Then it gradually decreases and becomes steady at 21 mbar. If the rocket engine is started before pressure in vacuum chamber reaches favourable conditions (at-least 0.1 bar), then flow separation may occur. Therefore it becomes essential to do a transient analysis to find out when minimum pressure is obtained. Data at two different points in the facility (one inside the Vacuum chamber and the other in the Nozzle) have been taken.

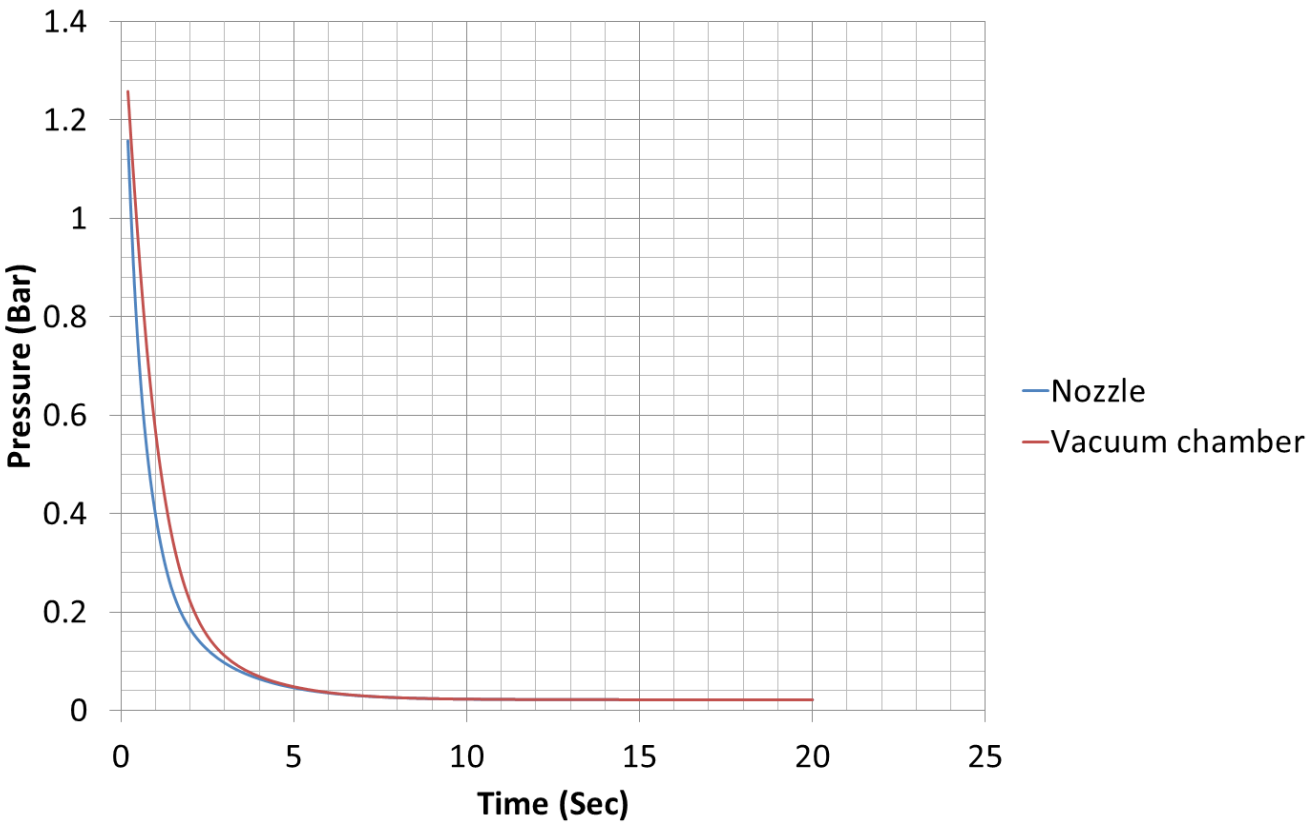


**Graph 4-15: Pressure drop vs Ejector start-up time**

The following observations have been made from graph 4-15:

- Pressure at both the places are slightly different until 4 s
- pressure at both the places fall below 0.1 bar after 3 s
- Pressure achieves steady state at approximately 5 s

Therefore at least 5 s of run time is recommended before starting the Thrust chamber.

## 4.7 Thrust Chamber start up

The Thrust chamber takes 3 seconds to reach 98 % partial load and takes an additional 7 seconds to reach full load condition. The analysis is done for 3 seconds. The analysis was done with pressure based and density based solvers which yielded different results. From the figures 4-16 and 4-17, it can be seen that density based solvers capture flow separation and reattachment correctly. In pressure based solvers, when the flow detaches the it fails to reattach. Reattachment was observed only when inlet pressure was increased to a large extent (more than its maximum value).

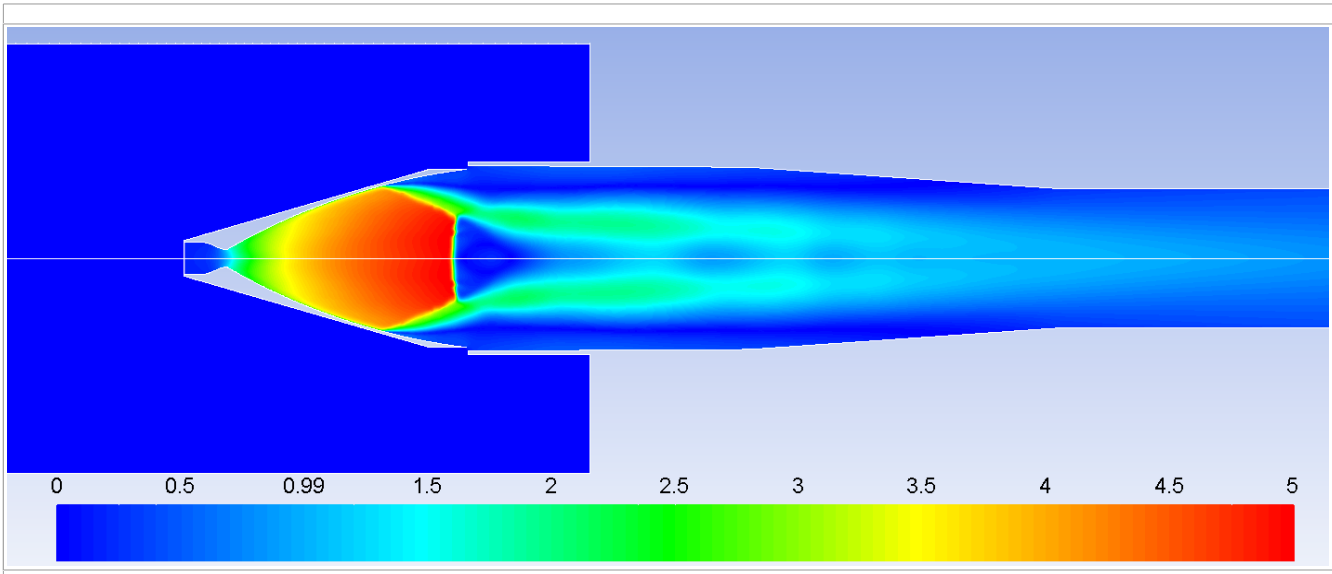


**Figure 4-16: Flow separation with pressure based solver at t=3 s**

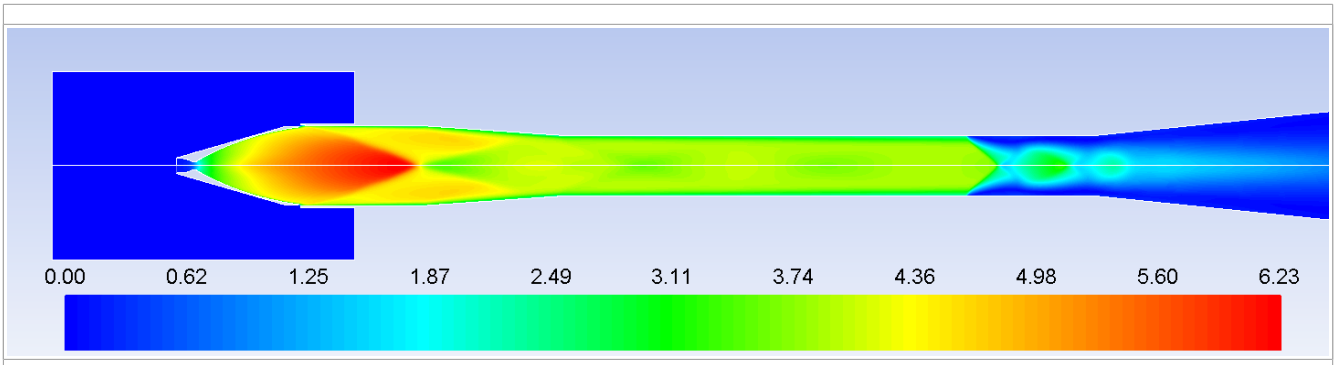


**Figure 4-17: No flow separation with density based solver at t=3 s**

Since the density based solver is accurate, it has been used in the rest of analysis. The following have been observed.

1. Nozzle flows full and Diffuser enters started condition at approximately same time at t=0.55

seconds when the vacuum chamber pressure is 62 mbar and the Nozzle is flowing at 11 bar . At this time the Mach reaches 96% of maximum value it can reach during the test. This is shown in the figures 4-18 and 4-19.

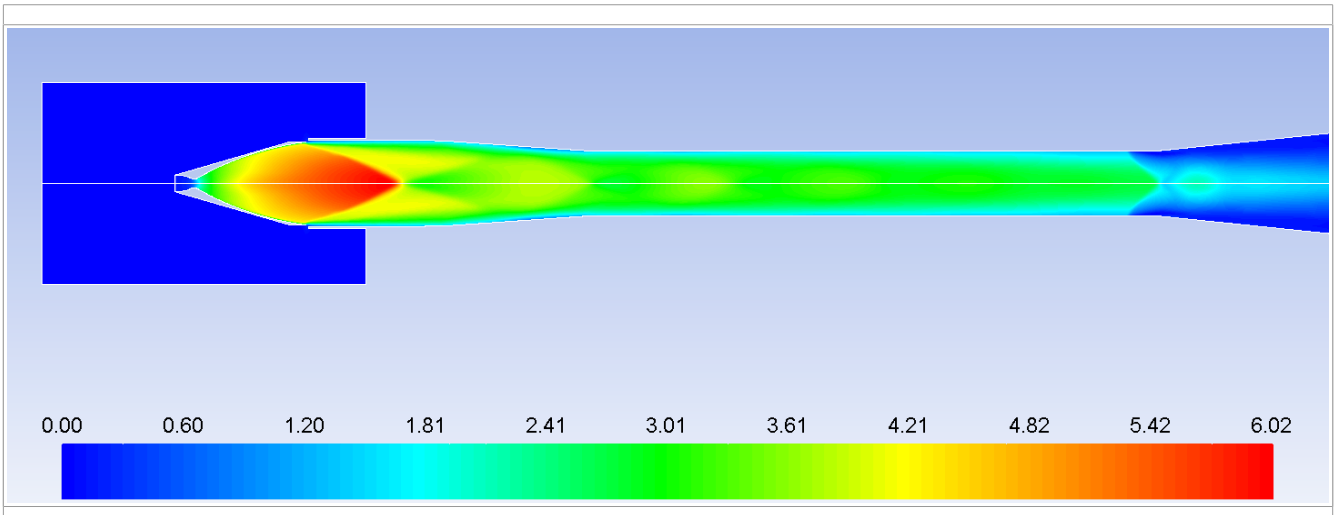


**Figure 4-18: Mach contours during engine start up at t=0.6 s**

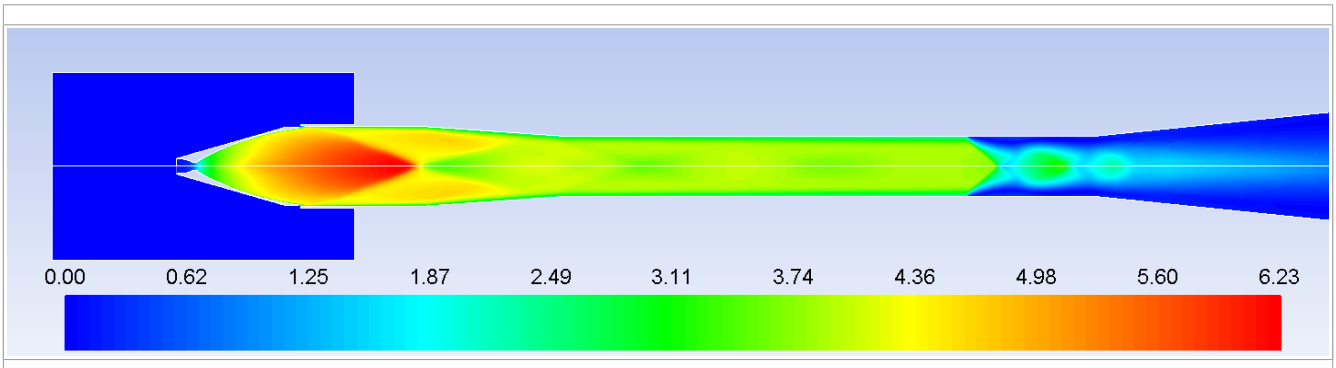


**Figure 4-19: Mach contours during Engine start up at t=3 s**

2. The Vacuum chamber is at ambient condition during the start up, the Diffuser flows at 50 % of the hot gas temperature, whereas the rest of the facility is almost equal to hot gas temperature. The Ejector section flows at a range of temperatures. It flows at maximum temperature at the walls and minimum temperature at its core where there is Nitrogen. This can be seen in the figures 4-20 and 4-21.

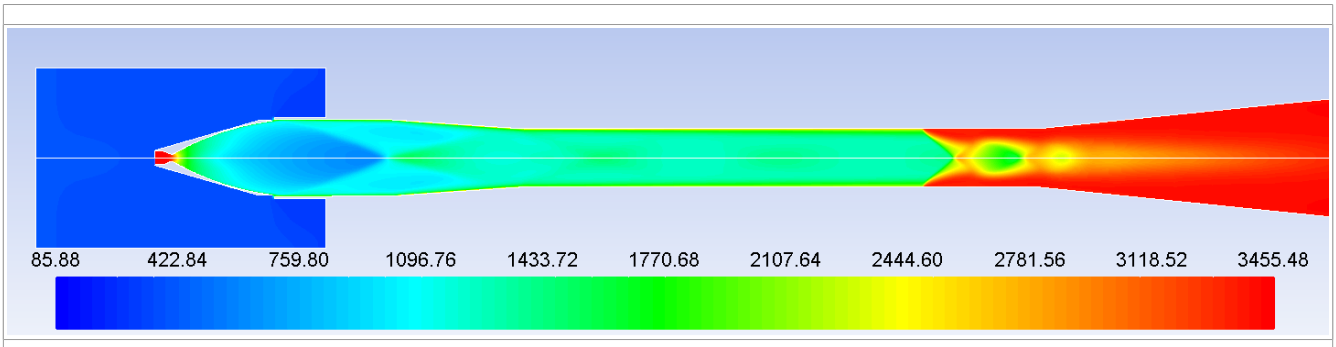


**Figure 4-20: Temperature contours during Engine start up at t=3 s in the Diffuser**

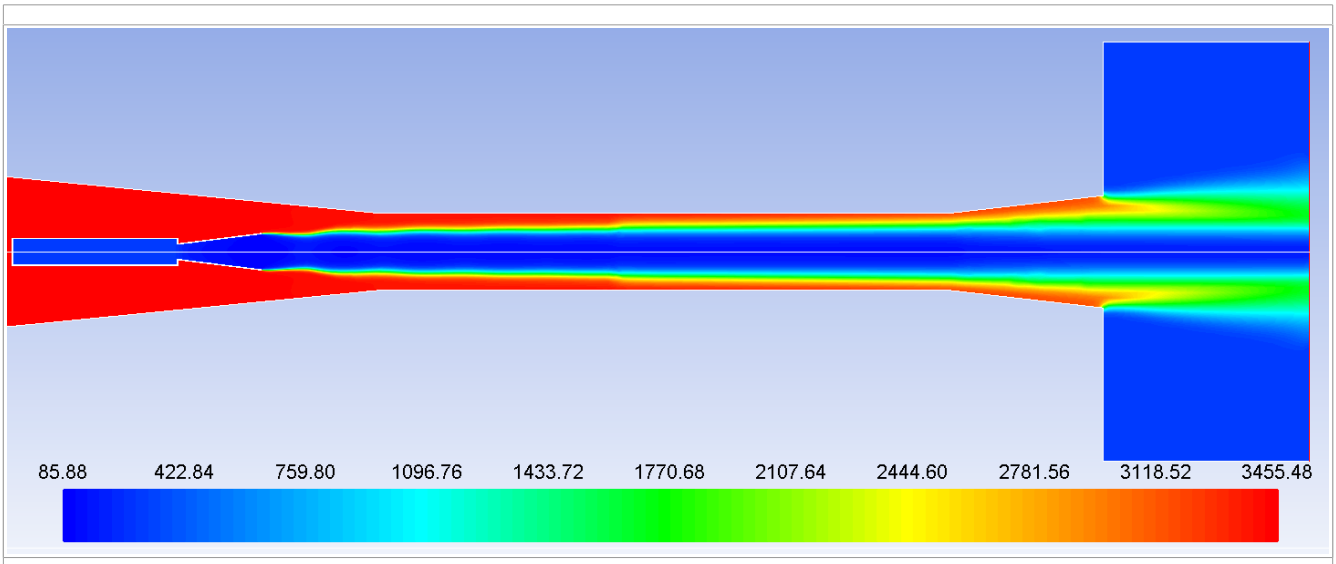


**Figure 4-21: Temperature contours during Engine start up at t=3 s in the Ejector**

3. When the Nozzle flows full there is minimum or no leak of flow into the Vacuum chamber as shown in figure 4-22. It forms a boundary layer when the flow detaches from the nozzle walls and smoothly attaches to the walls of Diffuser. Since no recirculation zone is formed, there is continuous entrainment from the vacuum chamber into the flow. This is an indication that annular gap and radial gaps are designed well.

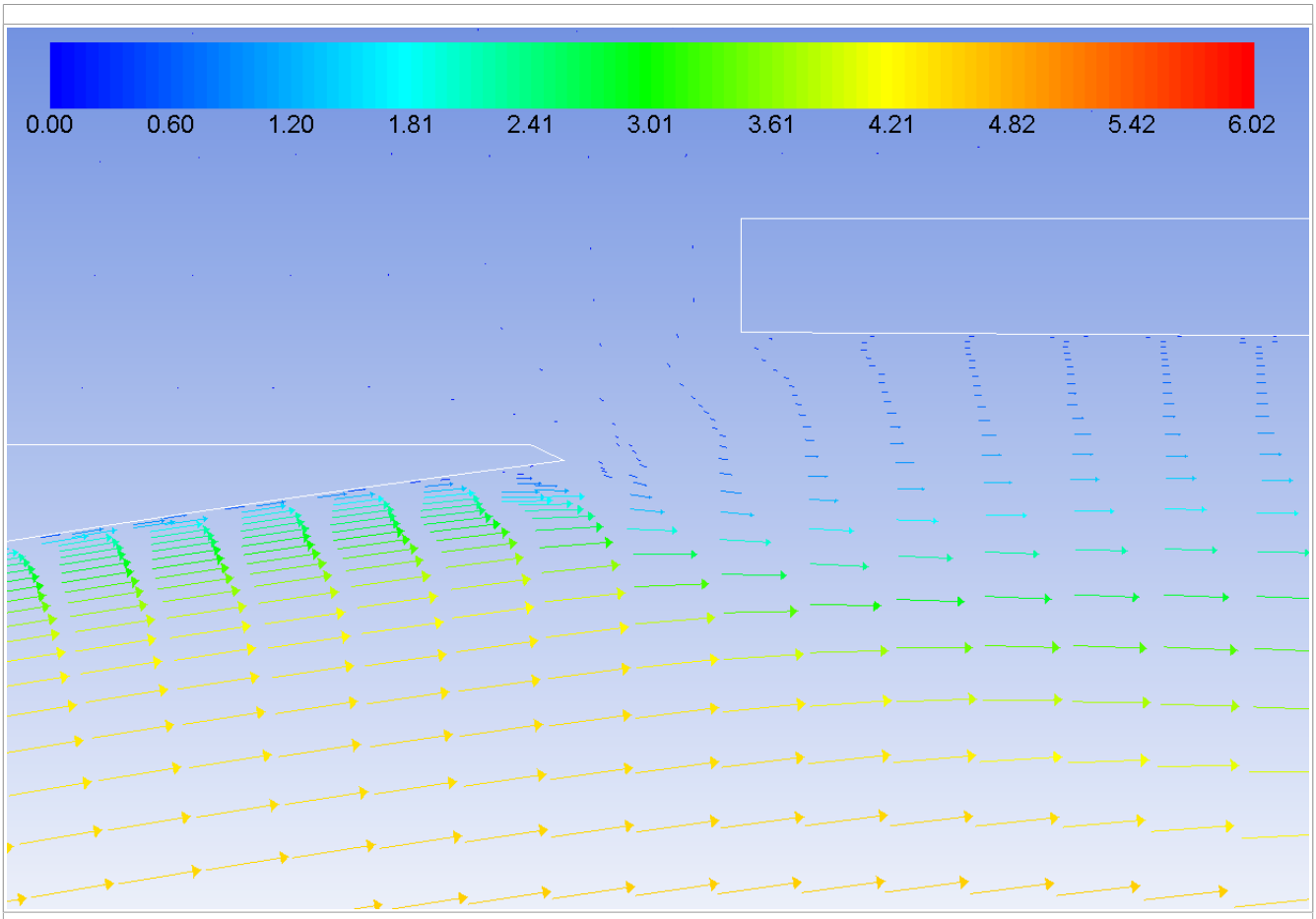


**Figure 4-22: Vectors of Mach during Engine start up at t=0.6 s**

## 4.8 Thrust chamber steady state

Diffuser flows at 50 % of the hot gas temperature, whereas the rest of the facility is almost equal to hot gas temperature. The Ejector section flows at a range of temperatures. It flows at maximum temperature at the walls and minimum temperature at its core where there is Nitrogen. All characteristics of temperature are similar to that of during Engine start up except that now the Vacuum chamber is at hot gas temperature as shown below. This high temperature indicates the need for water cooling.

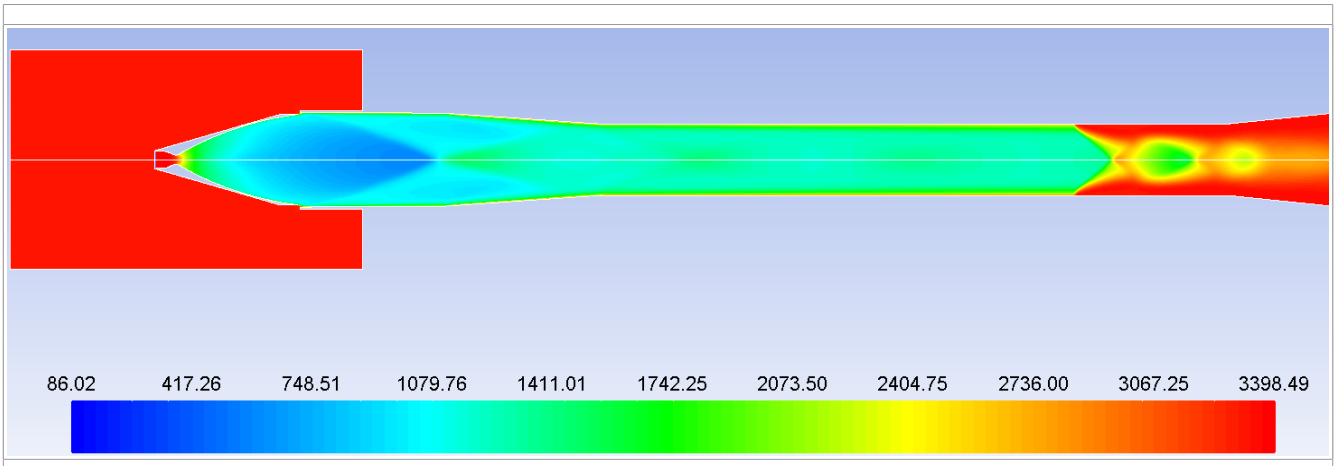


**Figure 4-23: Temperature contours at Engine started condition**

The Thrust chamber shows minor or almost no deviation in performance with respect to Ejector on/off condition after it reaches steady state.

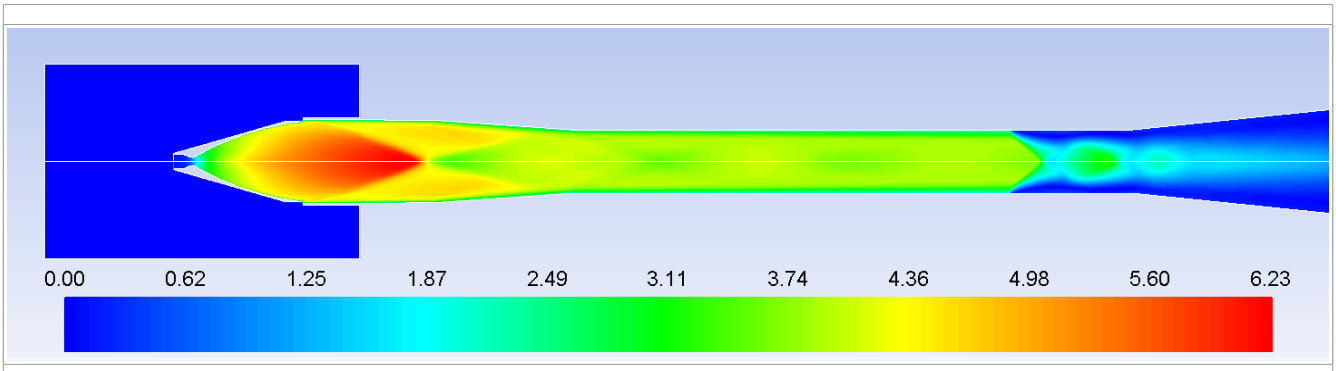


**Figure 4-24: Mach contours with Ejector off condition**

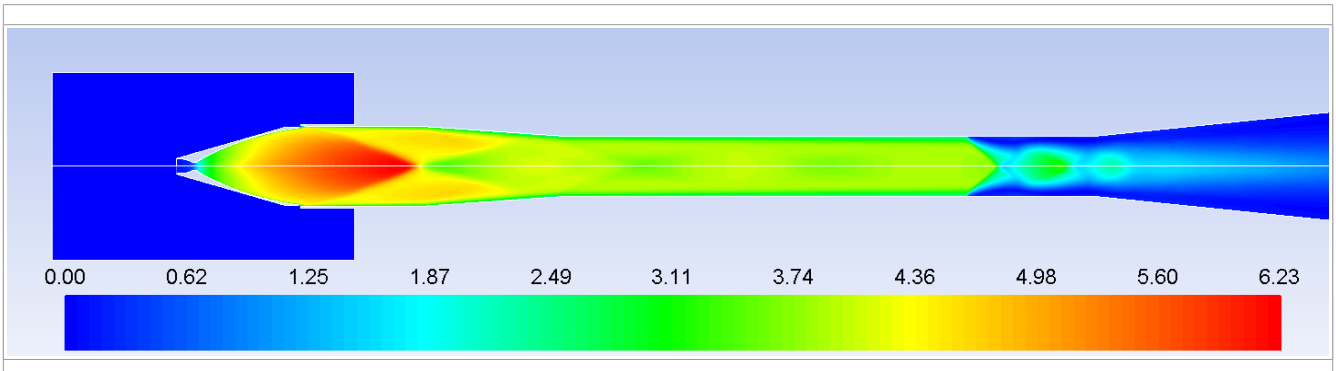


**Figure 4-25: Mach contours with Ejector on condition**

## 4.9 Thrust chamber shut down

The Thrust chamber takes 4.5 seconds to reach no load from full load condition. This analysis was done with both Ejector on and off conditions. The observations noted are:

1. Flow separation happens very early in case of Ejector off condition at t=0.45 seconds as seen below. During separation, pressure in vacuum chamber is 0.12 bar and thrust chamber flows at 38.5 bar. Since the ejector is in off condition the pressure in the rest of the facility is already equal to that of atmospheric pressure.

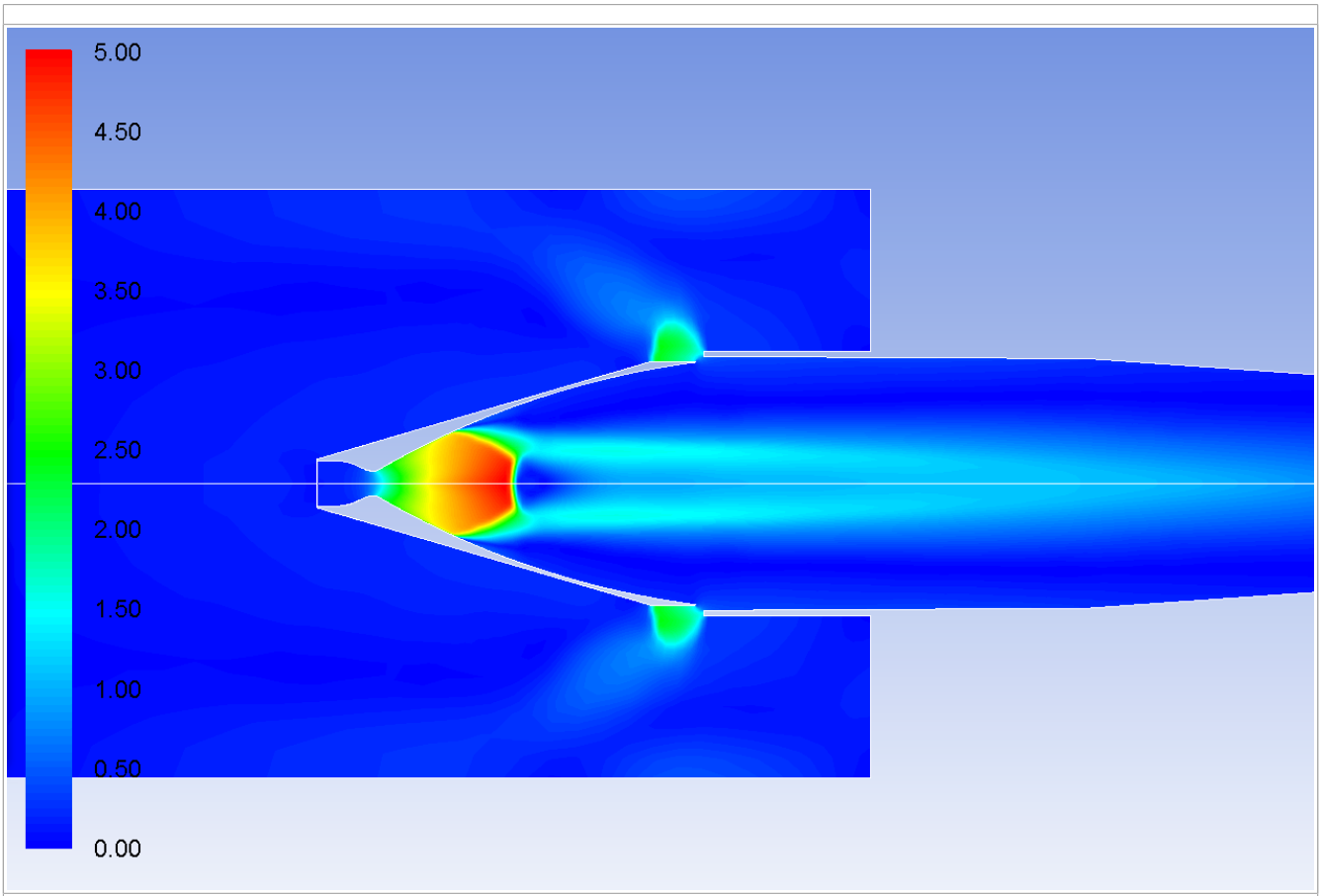


**Figure 4-26: Mach contours during engine shut down at t=0.45 s**

Flow separation happens a little late in case of Ejector on condition at t=2.35 seconds as seen in figure 4-27, and pressure in vacuum chamber is 0.03 bar while the thrust chamber flows at 10.3 bar. While the nozzle is at full load, its flow tries to suppress Ejector flow. Exhaust gas flows like an annular ring with Nitrogen flow at its core in the Ejector section. There is some mixing too. As the Thrust chamber shuts down, Nitrogen begins to dominate the Nozzle flow and in this process fills up the entire Ejector section cavity as seen in figures 4-28 and 4-29. This process helps to consistently maintain the vacuum in the

facility.

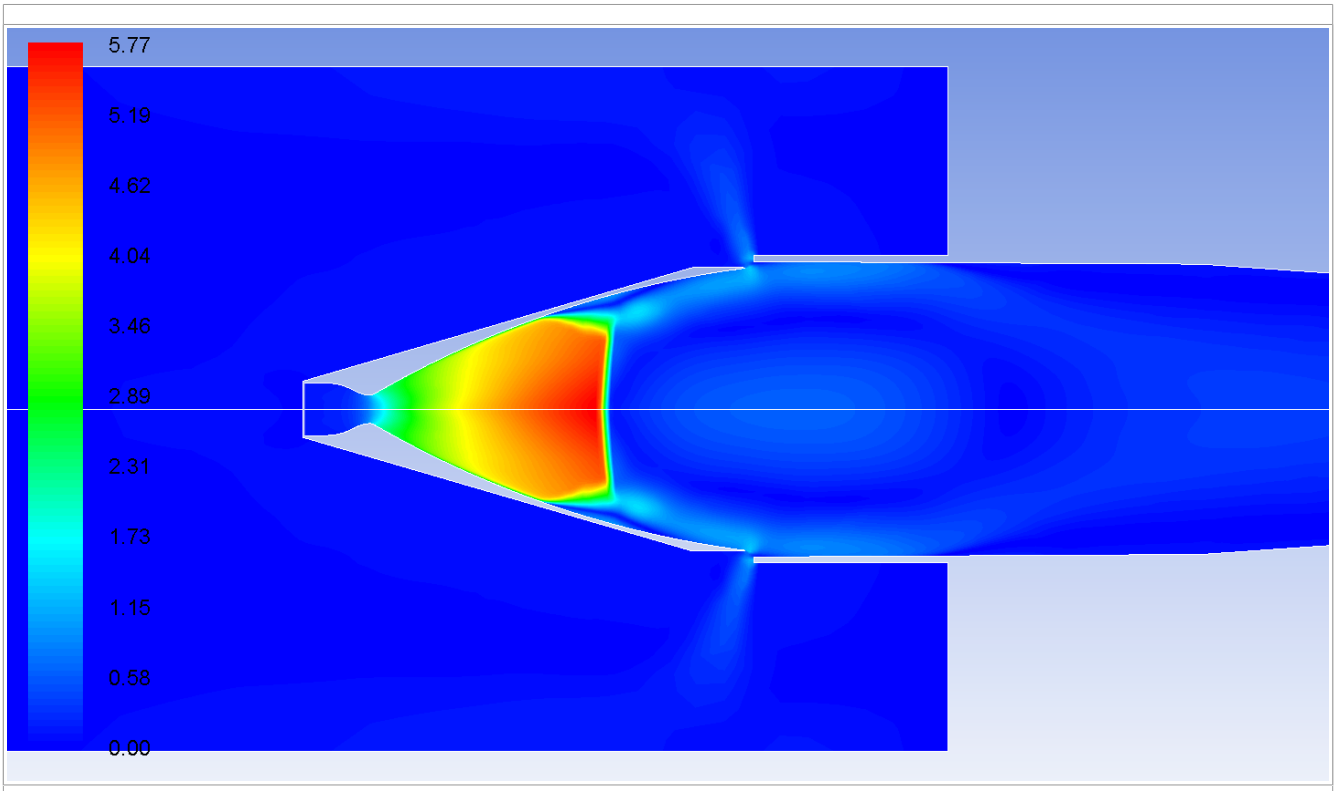


**Figure 4-27: Mach contours during Engine shut down with Ejector on at t=2.35 s**

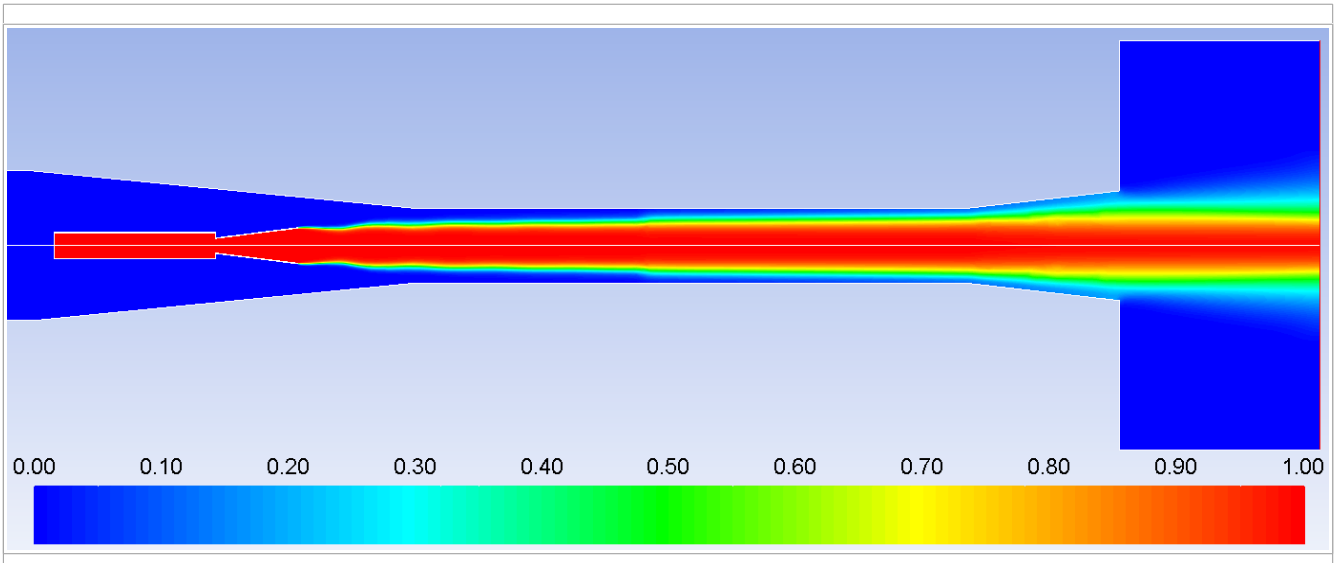


**Figure 4-28: Contours of nitrogen during Engine shut down at t=0.1 s**

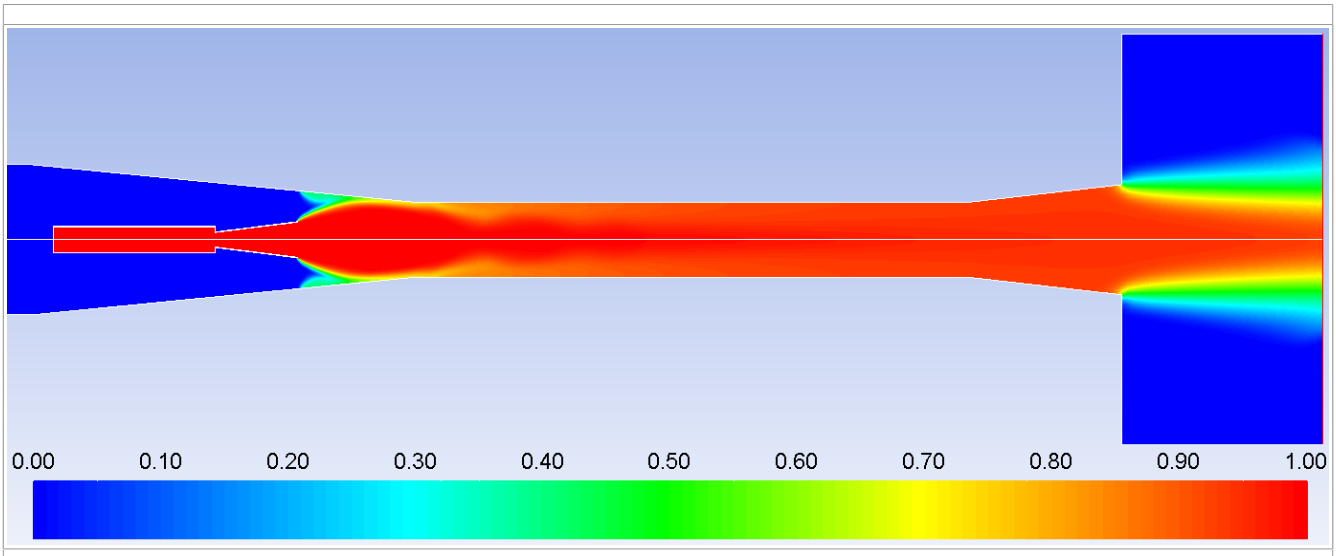


**Figure 4-29: Contours of Nitrogen during Engine shut down at t=3 s**

2. Separation in case of Ejector off is more aggressive than the other. This can be said so because a flow of M=3 flows into the vacuum chamber during Ejector off condition as shown in the figure 4-31 and M=1.8 flows during separation as shown in the figure 4-30.

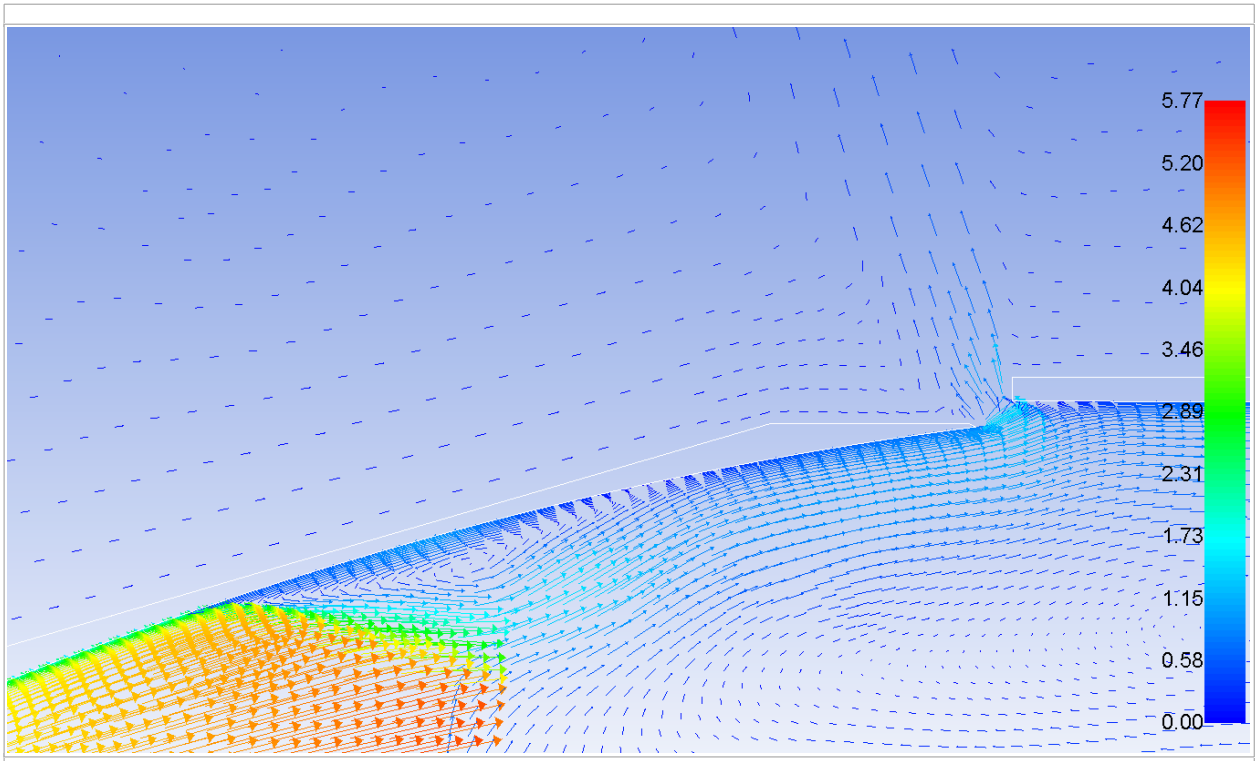


**Figure 4-30: Vectors of Mach during Engine shut down with Ejector on at t=2.35 s**

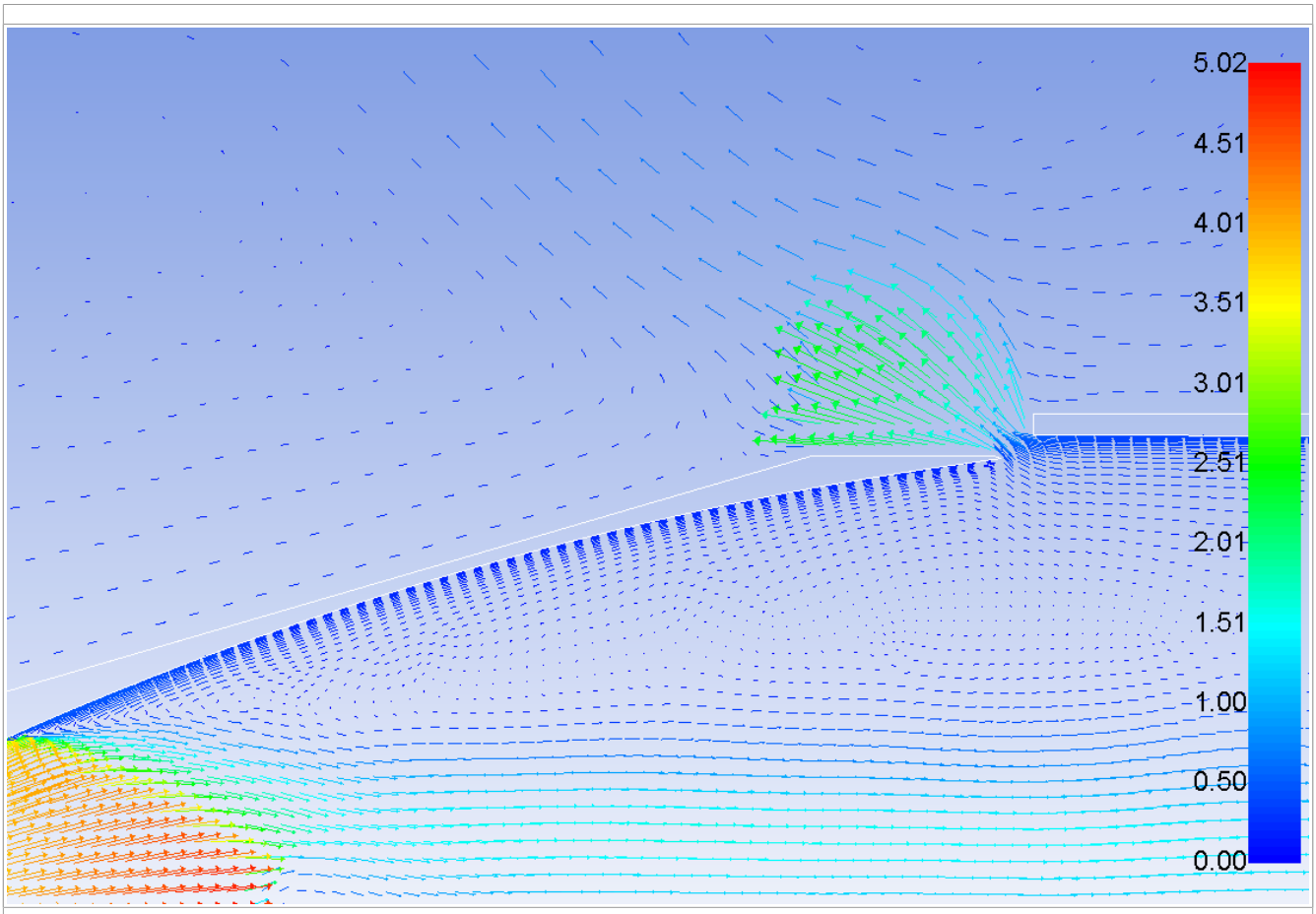


**Figure 4-31: Vectors of Mach during Engine shut down with Ejector off at t=0.45 s**

4. There is little or no re-entry of air in case of Ejector on condition as shown by the mole fraction contours of air in figure 4-32.

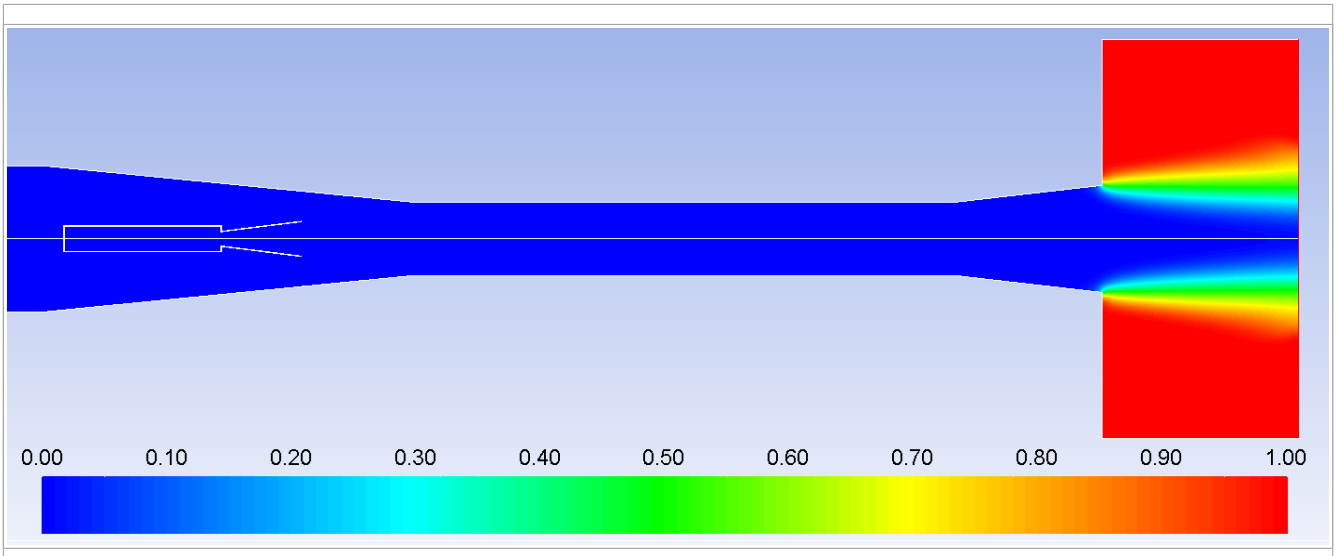


**Figure 4-32: Air during Engine shut down with Ejector on at t=5.35 s**

5. Figures 4-33 and 4-34 show air mole fraction at flow separation in Ejector off condition. Air re-entry starts at t=3 s and reaches the Ejector at 4.5 s. After that, it experiences resistance due to residual Nitrogen in the Ejector and slightly retracts. It resumes spreading into the facility at t=6.5 s. Hence Ejector off condition is not advisable during engine shut down period for safety reasons.

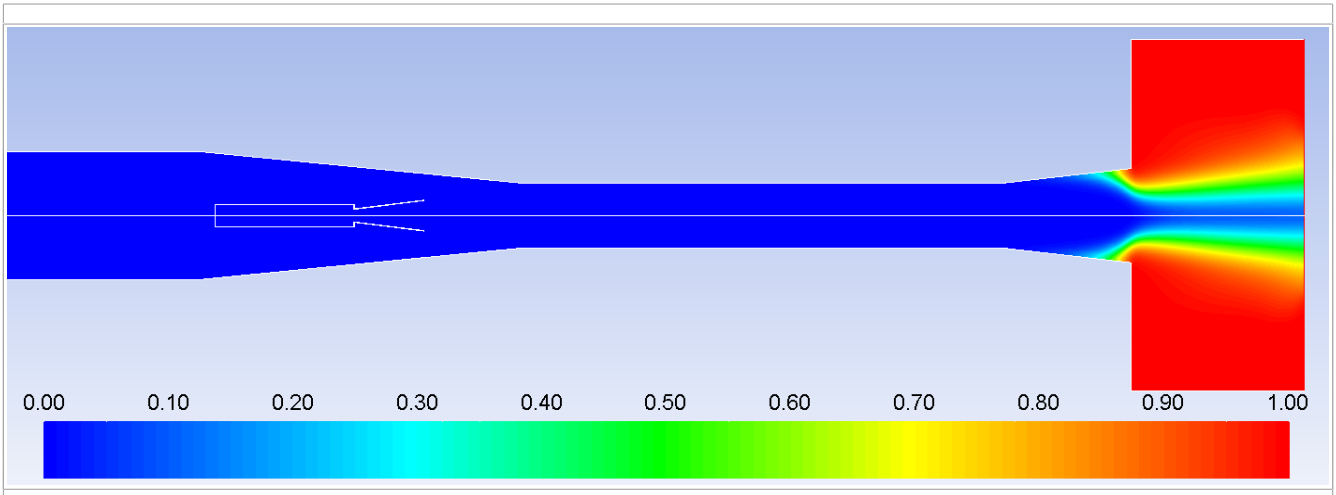


**Figure 4-33: Air re-entry at t=3s**

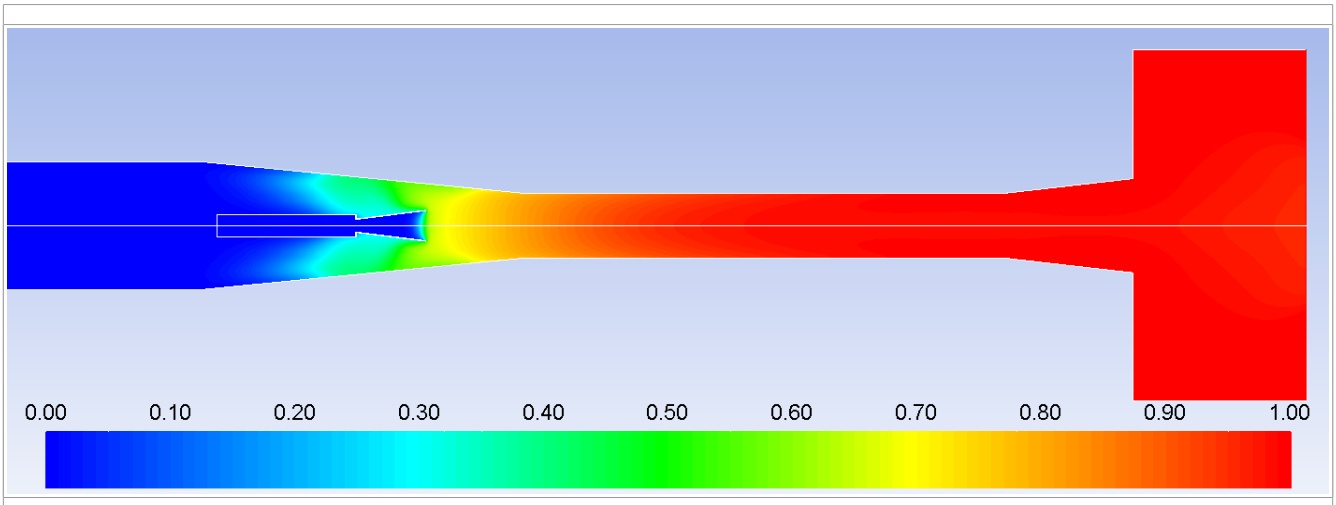


**Figure 4-34: Air re-entry at t=10.6 s**

# 5. Results and Discussion

This report has provided an insight over various aspects of CFD simulation and various components of the HAT facility. It has analysed the transient and steady state characteristics to provide critical information about flow dynamics, thermal aspects, vacuum creation and optimisation. The results can be summarised as:

1. Density based solvers are recommended over pressure based solver to capture shocks and flow phenomenon of high Mach flows.
2. K- ω (SST) turbulence model is recommended as it can predict flow separation with greater precision.
3. Optimum mass flow rate of Nitrogen from the Ejector is 340 kg/s. Steam is better than Nitrogen because its optimum flow rate is 270 kg/s.
4. Lesser molecular weight gases produce better vacuum conditions. This makes Methane the best fluid for ejector, but it is not recommended because steam is relatively abundant, easy to manufacture and environmental friendly.
5. Thrust chamber takes 0.55 seconds to reach 96% load condition.
6. Diffuser flows at 50% maximum temperature at all times.
7. After the Nozzle flow reaches steady state, Ejector may be switched off as it shows no influence on the latter.
8. During shut down, flow separation happens more early and aggressively in Ejector off condition than in on condition. Hence Ejector can be switched on prior to Engine shut down.
9. There is no back flow of air into the facility during shut down while the Ejector is on.
10. Back flow of air starts at 3 seconds and reaches the ejector at 7.5 seconds during Engine shut down while the Ejector is off. Hence for preventing the entry of air into the Diffuser section, Ejector can be switched on prior to shut down. This is mandatory for safety.

# References


[1] **Sutton and Larz;** *Rocket Propulsion Elements*

[2] *Liquid Rocket Engine Nozzles,* NASA SP-8120, July 1976

[3] **Leon Morisette, Thoedere Goldberg;** *Turbulent flow separation criteria for over-expanded supersonic nozzles,* NASA Technical paper 1207, August 1978.

[4] **K. Annamalai, K. Visvanathan, V. Sriramulu and K. A. Bhaskaran;** *Evaluation of the performance of supersonic exhaust Diffuser using scaled down models,* Experimental Thermal and Fluid Science, Volume 17, Issue 3, July 1998.

[5] **J. N. Sivo, C. L. Meyer and D. J. Peters;** *Experimental Evaluation of Rocket Exhaust Diffusers for Altitude Simulation*, Technical note D-298, NASA, July 1960.

[6] **L. Quebert and Y. Garcia;** *Theoretical and Experimental Design of an Exhaust Diffuser for an Upper Stage Engine of a Ballistic Missile*, 37 Joint Propulsion Conference and exhibit, AIAA 2001-3382.

[7] **M. R. Otterstatter, S. E. Meyer, S. D. Heister, E. M. Dambach;** *Design of an Altitude testing Facility for Lab-Scale Propulsion Devices,* 43 AIAA/ASME/SAE/ASEE Joint Propulsion Conference and exhibit, AIAA 2007-5323.

[8] **Nickey Raines and Bryon Maynard;** *A presentation on - Altitude Testing of large Liquid Propellant Engines,* 26 AIAA Aerodynamic Measurement Technology and Ground Testing Conference, AIAA 2008-3700.

[9] **Casey K. Kirchner;** *Design Evolution and Verification of the A-3 Chemical Steam Generator,* 45 AIAA/ASME/SAE/ASEE Joint Propulsion Conference and exhibit, AIAA 2009-5066.

[10] The brochure of – Glenn Research Test Facilities

[11] Status report 2011 – Institute of Space Propulsion, Lampoldshausen

[12] http://global.jaxa.jp/about/centers/kspc/

[13] http://www.kspc.jaxa.jp/english/tf/hats.html

[14] **Jan Ostlund;** *Flow process in Rocket engine nozzles with focus on low separation and side loads,* Stockholm, 2002, ISSN 0348-467X.

[15] **Robert H. Schmucker;** *Status of flow separation prediction in Liquid Propellant Rocket Nozzles,* Marshall Space Flight Centre, NASA, 1974, NASA-TM-X-64890.

[16] **R. Manikanda Kumaran, T. Sundararajan, D. Raja Manohar;** *Simulations of High Altitude Tests for Large Area Ratio Rocket Motors,* AIAA Volume 51, Number 2 (2013) .

[17] **Fanshi Kong and Heuy Dong Kim;** *Starting transient simulation of a vacuum ejector diffuser system under chevron effects,* 10 International Conference on Heat Transfer, Fluid

Mechanics, Thermodynamics, July 2014.

[18] **Alan Vincent E V**; CFD Analysis of Supersonic Exhaust Diffuser System for Higher Altitude Simulation.

[19] **R. Manikanda Kumaran, T. Sundararajan, D. Raja Manohar;** *Simulations of High Altitude Tests for Large Area Ratio Rocket Motors,* AIAA Volume 51, Number 2 (2013) .

[20] **Daniel Allgood, Jason Graham, Vineet Ahuja, Ashvin Hosangadi; Computational** *Analyses in support of sub-scale Diffuser testing for the A-3 Facility -Part I: Steady Predictions,* 45 AIAA/ASME/SAE/ASEE Joint Propulsion Conference and exhibit, August 2009, AIAA 2009-5204.

[21] **S. Sarkar, B. Erlebacher, M. Hussaini and H. Kreiss;** *The Analysis and Modelling of Dilatation Terms in compressible Turbulence,* Journal of Fluid Mechanics, Volume 227, April 2006.

[22] **Hyo-Won Yeom, Sangkyu Yoon, Hong-Gye Sung**; *Flow dynamics at the minimum starting condition of a supersonic diffuser to simulate a rocket's high altitude performance on the ground,* Journal of Mechanical Science and technology, October 2008, Springer.

[23] **Liu Daxiang, Zhou Hanzhong;** *China's High Altitude Test stand for Aircraft Engine under construction.*

[24] **N.S. Dougherty;** *Liquid Rocket Engine Testing - Historical Lecture: Simulated Altitude Testing at AEDC.*

[25] **Bauer, R. C. , and German, R. C.** ; *The Effect of Second-Throat Geometry on the Performance of Ejectors without Induced Flow,* Arnold Engineering Development Centre, November 1961.

[26] **Jones, W. L. , Price, H. S. , and Lorenzo, C. F.** ; *Experimental Study of Zero-Flow Ejectors Using Gaseous Nitrogen,* NASA 1960.

[27] **Manikanda Kumaran R, Vivekanand P K, Sundararajan T, Balasubramanian S, Raja Manohar D ;** *Analysis of Diffuser and Ejector Performance in a High Altitude Test Facility,* 26 AIAA, Applied Aerodynamic Conference, Hawaii.

[28] **J. H. Panesci and R. C. German**; *An analysis of second-throat diffuser performance for zero-secondary-flow ejector systems,* Arnold Engineering Development centre, December 1963.

[29] **Bartosiewicz, Y., Aidoun, Z., Desevaux, P., and Mercadier, Y.;** *Numerical and Experimental Investigations on Supersonic Ejectors,* International Journal of Heat and Fluid Flow, Volume 26, Issue 1, February 2005.

[30] **Reneau, L. R., Johnston, J. P. and Kline S. J.;** *Performance and design of straight, two dimensional diffusers,* ASME, Journal of Basic Engineering, Volume 89, Issue 1, November 2011.

[31] **Merkli, P. E., and Abuaf, N.;** *Flow Starting Times in Constant-Area Supersonic Diffusers,* AIAA Journal, Volume 15, Number 2, 1977.

[32] **Manikanda Kumaran, R., Vivekanand, P. K., Sundararajan, T., Kumaresan, K., and Raja Manohar, D.;** *Optimization of Second Throat Ejectors for High Altitude Test Facility,* Journal of Propulsion and Power, Volume 25, Number 3, 2009.

[33] **Mikhail Pavlovich Bulat and Pavel Victorovich Bulat;** *Comparision of Turbulence Models in the calculation of Supersonic Separated flows,* World Applied Science Journal 27, 2013, ISSN 1818-4952.